American College of Radiology™

2025 ACR® Medical Student Research Fair Abstract Book

Dear Readers,

It is a privilege to share with you the inaugural edition of the ACR Medical Student Research Symposium Abstract Book. This collection represents the dedication, creativity, and perseverance of medical students across the country who have chosen to explore important questions in radiology and healthcare. Each abstract reflects the hard work and curiosity that drive our field forward.

This year's projects span a wide range of themes, from clinical and translational research, to health systems and quality, to case reports, education, and the growing role of artificial intelligence in radiology. The diversity of work included here highlights not only the broad reach of radiology but also the unique perspectives that medical students bring to the specialty.

This book is also a testament to collaboration. We are grateful to the faculty mentors who guided students in their projects, to the keynote speakers who have generously shared their time and insights, and to the ACR community for fostering an environment where students can learn, contribute, and grow. I would like to especially thank Dr. Pamela Woodard for her continued support of this symposium and for generously reviewing this abstract book, and Dr. Elahi for her encouragement and mentorship of students. Their leadership, alongside that of many others in the radiology community, continues to inspire us.

I am deeply appreciative of our planning team, who worked tirelessly to bring this project together, and of every student who submitted their work. Your efforts ensure that this symposium is not only an event but a lasting contribution to the academic community.

It is my hope that this abstract book will serve as a resource, a source of inspiration, and a reminder of the bright future of radiology. Thank you for joining us in celebrating student research, and we look forward to seeing how these projects will continue to grow and evolve.

Sincerely,

Ahmed Salti, BS

Editor, ACR Medical Student Research Symposium Abstract Book

DO Candidate, 2027

Keynote Speakers

Pamela Woodard, MD, FACR

Fatima Elahi, DO, MHA

Student Oral Presentation Finalists

Trevor M. Canty, BA

Saumith R. Bachigari, BS

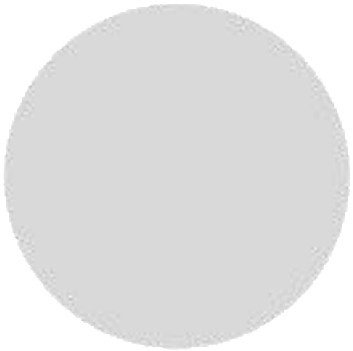

Deeptha Bejugam, BS

Jacob Divine, BS

Julia Liu, BSc

Qays Abu-Saymeh, BS

2025 ACR Medical Student Symposium Planning Team

Fayhaa Doja, BS
Co-lead

Sydney Gibson, BS
Co-lead

Dave Patel
Co-moderator

Ahmed Salti
Co-moderator

Hreedi Dev, BA

Monica Lee, DO

Christine Liu, BS

Jocelyn Selan, MS

Nola Vu, BA

Table of Contents

Clinical & Translational Research

Comparison of Percutaneous Ultrasound-Guided Versus Image-Guided Transjugular Liver Biopsies in Post-Hepatic Transplant Patients: An 8-Year Retrospective Review of Outcomes and Complication Rates

Pasha Pourebrahim, BA[2], Hubert Smith, MD[1], Alina Corona, MD[2], Blake Taurone, MD[2], Saher Sabri, MD[1], David Field, MD[1]
[1]Department of Radiology, MedStar Georgetown University Hospital
[2]Georgetown University School of Medicine

Introduction:

Liver biopsy remains the gold standard for evaluating graft function following liver transplantation, enabling diagnosis of allograft rejection, recurrent disease, ischemic injury, and biliary complications. Two primary image-guided techniques are employed: percutaneous liver biopsy (PLB) and transjugular liver biopsy (TJLB). PLB is generally favored due to faster procedural times and lack of ionizing radiation, whereas TJLB is preferred for patients with coagulopathies or ascites. At many institutions, TJLB is selected during the early post-transplant period due to perceived safety benefits, although comparative data remain limited. This study aimed to compare hemorrhage rates and biopsy yield between PLB and TJLB in transplant recipients eligible for either technique.

Methods:

A retrospective cohort study was conducted involving all liver transplant recipients who underwent image-guided liver biopsy from 2014 to 2022 at a single tertiary center. Patients with contraindications to PLB, including elevated INR, thrombocytopenia, or large-volume ascites, were excluded. Data collected included patient demographics, time from transplant to biopsy, laboratory parameters, procedural complications, and adequacy of biopsy specimens. Subgroup analysis was performed for patients biopsied within 90 days post-transplant. Hemorrhage requiring transfusion or additional intervention and biopsy yield were the primary endpoints. Statistical comparisons were performed using chi-square and t-tests; significance was defined as $p \leq 0.05$.

Results:

A total of 814 transplant recipients met inclusion criteria: 503 underwent PLB and 311 underwent TJLB. The overall post-procedural hemorrhage rate was 0.74% (6/814), with a significantly higher rate observed in the TJLB group (1.6%) compared to the PLB group (0.2%) ($p = 0.033$). Biopsy adequacy was high in both groups, with sufficient tissue obtained in 99.4% of PLB cases and 99.7% of TJLB cases ($p = 1.0$). Time from transplant to biopsy was significantly longer in the PLB group (median 54.8 months vs. 40.1 months; $p < 0.0001$). Among the 162 patients biopsied within 90 days post-transplant (58 PLB, 104 TJLB), no statistically significant differences in hemorrhage rate ($p = 0.55$) or biopsy adequacy ($p = 1.0$) were identified.

Discussion:

Both PLB and TJLB demonstrated favorable safety profiles and high diagnostic yield in transplant recipients eligible for either approach. The statistically higher hemorrhage rate in the TJLB group contrasts with common assumptions regarding its superior safety in coagulopathic or early post-transplant patients. Subgroup analysis confirmed comparable outcomes between techniques even during the early post-transplant period.

Conclusion:

Image-guided percutaneous and transjugular liver biopsies are both safe and diagnostically effective in post-transplant patients without contraindications to either method. Findings support the use of PLB in select early post-transplant cases, with implications for procedural efficiency and reduced radiation exposure. Institutional practices favoring TJLB in the immediate post-transplant setting may warrant reconsideration in light of these results.

The Cardiovascular Impact of Rheumatoid Arthritis: A Systematic Review of Coronary Artery Calcification Within Rheumatoid Arthritis Patients

Stephanie Nagy, BScN[1], Daniel Naus, MS[1], Alejandro Biglione, MD[2]
[1]Nova Southeastern University
[2]Internal Medicine, Wellington Regional Medical Center, Wellington, USA

Background:

Worldwide, rheumatoid arthritis (RA) is the leading inflammatory arthropathy. The musculoskeletal impacts of RA are well known; however, the inflammatory nature of the disease extends beyond the joint synovium. The cardiovascular system is the most impacted within RA patients and is the leading cause of death within this vulnerable group. Recently, coronary artery calcium (CAC) score has become a popular method to analyze the calcifications within the coronary vessels.

Methods:

A review was performed using CINAHL, OVID, EMBASE, and Web of Science. A total of 305 articles were screened, with 11 articles included. The studies were considered eligible if they involved CT coronary angiography in RA patients with no prior cardiovascular disease and no prior or current use of lipid-lowering medications.

Results:

1141 patients with RA, with a mean disease duration of 127.7 months. The majority of patients were females, 78.4%, with a mean age of 56.9. 59.3% of RA patients reported an elevated CAC score above 0 Agatston units, which indicates calcified plaque deposits in the coronary vessels. Of those, 40% were found to have moderate to severe calcification of over 100 Agatston units. Furthermore, a synergistic relationship may exist between elevated levels of the rheumatoid factor (RF) and anti-cyclic citrullinated peptide (ACP), plaque deposition and coronary vascular disease.

Discussion:

Invasive coronary angiography is considered the gold standard for diagnosing cardiac abnormalities, but non-invasive CT coronary angiography has gained popularity in recent years due to its low-risk nature and ability to identify calcifications within the plaque. RA induces a proinflammatory state in the body by elevating tumor necrosis factor-alpha, interleukin-1, and interleukin-6, which contribute to atherogenesis. Additionally, it increases reactive oxygen species, leading to endothelial damage and plaque buildup. Most patients with RA analyzed in this review were positive for RF and/or ACP, which not only indicates a prominent inflammatory state, but it can also be tied to independent risk factors of atherogenesis. Research efforts have suggested that citrullinate epitopes within the atherosclerotic plaque are targets for ACPA, leading to autoimmune inflammation in the vessels and further calcified plaque buildup. As a result, it is crucial to conduct

timely cardiovascular lipid screening, as well as CT angiography, in patients with RA to monitor for plaque deposition and progression.

Conclusions:

As medicine shifts to a preventative rather than a reactive focus, it is crucial to alter clinical practice guidelines to include monitoring for systemic impacts, especially within the cardiovascular system. It also highlights the crucial role that CT coronary angiography can have in identifying the higher prevalence of coronary artery calcification in RA patients. Identifying elevated CAC scores in RA patients can prompt aggressive management of cardiovascular risk factors prior to the progression of more severe negative outcomes, leading to enhanced patient outcomes.

Murine Brain Networks Induced by Selective Stimulation of TRPA1 Vagus Nociceptors

D.C. Lee[1,2], A. Torres[1], O. Hashimoto[1], S.S. Chavan[1,2,3], K.J. Tracey[1,2,3]
[1]Institute for Bioelectronic Medicine, Feinstein Institutes for Medical Research, Northwell Health, 350 Community Drive, Manhasset, New York 11030, USA
[2]Donald and Barbara Zucker School of Medicine at Hofstra/Northwell, 500 Hofstra University, Hempstead, New York 11549, USA
[3]The Elmezzi Graduate School of Molecular Medicine, 350 Community Drive, Manhasset, New York 11030, USA

Introduction:

The inflammatory reflex involves afferent and efferent vagus nerve fibers as a physiological interface between the brain and the inflammatory response. Activation of Transient Receptor Potential Ankyrin-1 (TRPA1)-expressing vagus nociceptors has been previously shown to activate the afferent arc of this reflex. We hypothesized that TRPA1-signaling in the vagus nerve would activate specific neuronal ensembles in the brain.

Methods:

To label neuronal populations activated by TRPA1 signaling, we created Targeted Recombination-in Active Populations (TRAP2)-tdTomato mice by crossing TRAP2 mice with a Cre-dependent tdTomato reporter line. When these mice are exposed to 4-hydroxytamoxifen, active neurons persistently express the fluorescent protein tdTomato. Vagus TRPA1 fibers were stimulated opto-pharmacologically using optovin and 405 nm light, and tdTomato expression in the brain was subsequently assessed. Images were taken utilizing serial two-photon tomography imaging (STP) for 3D rendering of the murine brain to identify activated brain regions and neurons. The number of tdTomato+ cells was manually quantified in select brain regions with known association with either TRPA1 stimulation or vagus nerve stimulation. Optovin-stimulated groups (n=3) were compared to sham-stimulated control groups (n=3) and graded on a scale ranging from low activity (+) to high activity (++++).

Results:

We observed increased brain activity in the paraventricular nucleus of the hypothalamus and locus coeruleus.

Discussion:

These findings indicate that specific vagus TRPA1 nociceptors induce specific brain neuron activity. The methodology employed, combining TRAP2 and STPT, offers a novel protocol to screen for the activation of brain neurons in response to vagus TRPA1 signals.

Conclusion:

Our results demonstrate a technique that identified specific brain regions activated by TRPA1 vagus nociceptors, which can be applied to disease models and therapeutics to better enhance our understanding of their mechanisms. There is ample opportunity for translational application of computational tomography techniques utilized here to clinical tomography samples to better visualize and standardize images.

Resting-State Functional Connectivity Alterations in Bipolar Disorder: A Systematic Review – Meta Analysis of rs-fMRI Studies

Jay Kakadiya, MBBS[1], Beatriz Aguiar de Macedo, MD[1], Licia Pacheco Luna, MD, PhD[1]
[1]Johns Hopkins University School of Medicine, Russell H. Morgan Department of Radiology and Radiological Science, Baltimore, MD, USA

Introduction:

Bipolar disorder (BD) is a chronic psychiatric illness characterized by recurrent mood fluctuations and functional impairment, affecting up to 3% of U.S. adults. Resting-state functional MRI (rs-fMRI) is a key modality for examining functional connectivity (FC) abnormalities in BD, though findings remain inconsistent due to methodological variability. This study aims to synthesize rs-fMRI findings to identify consistent FC alterations and guide future research and clinical strategies.

Methods:

Following PRISMA guidelines, a systematic review was conducted using PubMed, EMBASE, and Scopus. Seventeen rs-fMRI studies met inclusion criteria and were categorized by analytic approach: independent component analysis (ICA), seed-based connectivity, graph-theory metrics, and others. Extracted data included participant demographics, imaging parameters, and FC findings. Coordinate-based meta-analysis was performed for whole brain studies using GingerALE.

Results:

Seventeen studies met inclusion criteria, comprising 1,899 participants (978 with BD and 921 healthy controls). Whole brain ICA studies reported altered FC in the left inferior frontal gyrus—pars triangularis and bilateral angular gyrus, and in the left precuneus/posterior cingulate cortex (PCC) and bilateral prefrontal cortex. A meta-analysis of eleven whole-brain studies identified a significant 2,544 mm^3 cluster (Fig-1) with increased FC encompassing the medial frontal gyrus ($p < 0.001$) and anterior cingulate cortex ($p < 0.001$). Seed-based studies found significant FC differences in the bilateral prefrontal cortex, bilateral precuneus/PCC, and medial frontal gyrus. Graph-theory and other methods revealed disruptions in the right precuneus/PCC and left medial frontal gyrus.

Conclusion:

Despite methodological variability, a consistent pattern of dysconnectivity is evident in core regions of the default mode network (DMN) and fronto-parietal network (FPN). Frequent involvement of the prefrontal cortex, precuneus/PCC, and angular gyrus suggests their central role in BD pathophysiology. These findings highlight potential neural targets for neuromodulation, biomarker development, and personalized treatment. Future research should adopt standardized protocols and larger, longitudinal designs to validate these networks as reliable markers of disease state and therapeutic response.

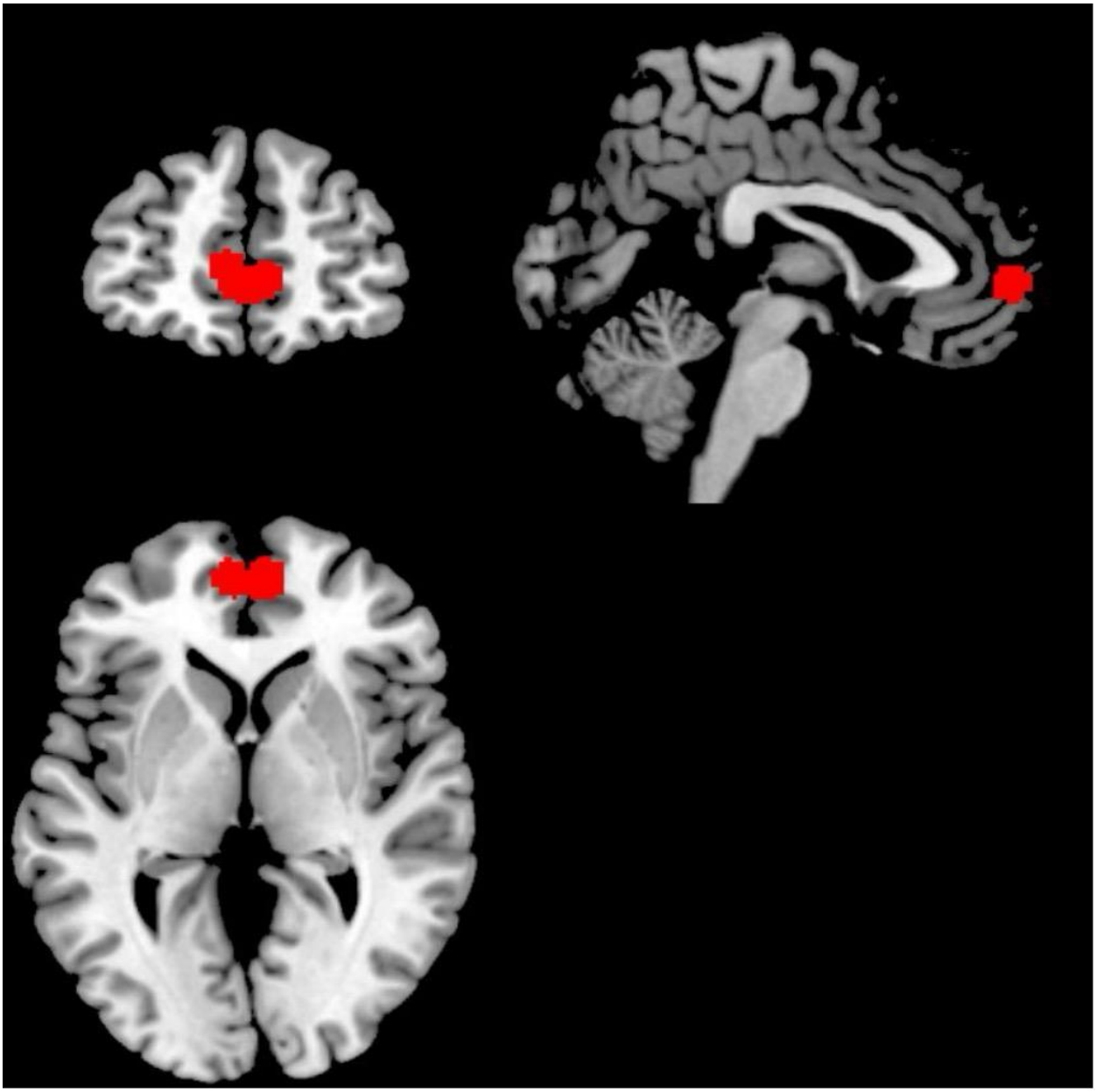

Figure 1. Regions in red indicate clusters with significantly increased functional connectivity ($p < 0.001$) in patients with bipolar disorder compared to healthy controls.

Brain Activation During Scene Encoding fMRI in the Alzheimer's Disease Continuum: Association with Amyloid and Tau Burden in PET

Mia S. Trueblood[1], Andrew J. Saykin[2,3], Shannon L. Risacher[2,3]
[1]Medical Scientist Training Program, Indiana University School of Medicine
[2]Department of Radiology & Imaging Sciences
[3]Indiana Alzheimer's Disease Research Center, Indiana University School of Medicine

Background and Hypothesis

This project assessed brain activation during a scene encoding task in 4 groups: older adults who were cognitively normal (CN), subjective cognitive decline (SCD), mild cognitive impairment (MCI), and dementia due to Alzheimer's disease (AD). Associations between scene encoding related brain activation and tau, amyloid, and other biomarkers were analyzed. Our hypothesis was that higher levels of cerebral tau and amyloid would be associated with reduced scene encoding activation. In addition, we hypothesized that scene encoding activation would be significantly different between cognitively normal and cognitively impaired groups.

Methods:

234 individuals from the Indiana Memory and Aging Study (79 CN, 67 SCD, 70 MCI, and 18 AD) completed structural and functional MRI, clinical/cognitive assessment and biomarkers; 155 underwent amyloid ([^{18}F]florbetapir/[^{18}F]florbetaben) PET, while 111 also underwent [^{18}F]flortaucipir PET. For the fMRI scene encoding task, participants were asked to view and remember a set of images. A one-way ANOVA test was used to analyze scene encoding related activation differences among the 4 groups. Regression was used to identify associations between scene encoding activation and tau and amyloid deposition.

Results:

Significant differences in activation were observed between the MCI and CN groups, including less activation in widespread regions during the task and reduced deactivation in the default mode network (DMN) in MCI participants relative to CN. Significant associations between higher amyloid and tau deposition and altered scene encoding activation were also observed.

Conclusion and Potential Impact:

Cognitive decline is associated with activation changes during scene encoding, as well as reduced deactivation in the DMN, especially in the posterior cingulate region. Higher cerebral amyloid deposition predicted decreased scene encoding related activation. These findings are consistent with models linking cognitive status, functional brain activation during episodic encoding, and pathophysiological processes in the AD continuum. The positive association with tau is a new finding that should be explored with further studies.

Detection of Osseous Spinal Metastases with T1-Weighted Dynamic Contrast-Enhanced Perfusion MRI and PET: Assessing Agreement with Positive Biopsy

Deeptha Bejugam, BS[1,2], Kyung K. Peck, PhD[2,3], Atin Saha, MD[2], Elena Yllera-Contreras, MD[2], Onur Yildirim, MD[2], Julio Arevalo-Perez, MD, PhD[2], Simone Krebs, MD[2], Eric Lis, MD[2], Sasan Karimi, MD[2], Andrei Holodny, MD[2]
[1]Georgetown University School of Medicine, Washington, D.C.
[2]Department of Radiology, Memorial Sloan Kettering Cancer Center, New York, NY
[3]Department of Medical Physics, Memorial Sloan Kettering Cancer Center, New York, NY

Introduction and Objective:

For patients suspected of having metastatic spinal lesions, ^{18}F-fluorodeoxyglucose (FDG) positron emission tomography (PET) and magnetic resonance imaging (MRI) are first-line imaging modalities. While conventional MRI provides morphological information, dynamic contrast-enhanced MRI (DCE-MRI) measures vascular perfusion parameters, including vessel permeability (K_{trans}) and plasma volumity (V_p), which are markers of viable tumors.[1,2] Although DCE-MRI and PET are individually recognized for detecting tumors, no prior comparisons between V_p and PET maximum standardized uptake value (SUV_{max}) have been performed. This study evaluates the concordance between PET and DCE-MRI in identifying pathologically confirmed, untreated osseous spinal metastases and assesses DCE-MRI's non-inferiority to PET.

Methods and Materials:

Non-treated osseous spinal metastases biopsy-confirmed between February 2015 and January 2022 with available DCE-MRI and ^{18}F-FDG PET/CT scans were retrospectively analyzed. Exclusion criteria included intervals exceeding one year between DCE-MRI and PET, recorded radiation therapy within two vertebrae of the lesion, and systemic therapy between DCE-MRI and PET. Mean *K*-trans and mean V_p were estimated in the lesion's region of interest (ROI) using an extended Tofts pharmacokinetic model with NordicICE software. SUV_{max}, adjusted for patient body weight and liver function, was obtained from the PET scans in the lesion's ROI. For DCE-MRI, a V_p threshold of 2.10 as determined in the literature was used to detect spinal metastases; lesions with a Vp of 2.10 or more were classified as true positives for viable tumors.[3] For PET, SUV_{max} thresholds of 2.00, 2.50, and 4.00 reported in the literature were examined.[4,5] Agreement between V_p and each SUV_{max} threshold was assessed, and McNemar tests ($\alpha = 0.05$) were used to determine any statistically significant differences in the number of metastases detected.

Results:

85 metastases across 69 patients (mean age: 64.15 ± 12.13; 35 men) were evaluated. At an SUV_{max} threshold of 2.00, V_p demonstrated a high agreement of 81.18% with SUV_{max} in detecting spinal metastases. Agreement with other SUV_{max} thresholds was lower, as expected. Compared to all 3 SUV_{max} thresholds, V_p identified the highest number of metastases ($p < 0.001$). Supplemental McNemar tests looking at 62 cases with DCE-MRI and PET scans within 1 month of each other

similarly found V_p identifying more metastases than SUV_{max} thresholds of 2.00, 2.50, and 4.00 ($p = 0.003$, $p < 0.001$, and $p < 0.001$, respectively).

Discussion:

In general, V_p from DCE-MRI and SUV_{max} from PET exhibit a good agreement in detecting osseous spinal metastases. However, when common thresholds of these metrics are applied, V_p outperforms SUV_{max} in identification of viable tumor. Our study shows that DCE-MRI plays a key role in detecting viable spinal metastasis, and in some instances, more accurately classifies tumor compared to PET.

Conclusion:

This study provides strong evidence for incorporating DCE-MRI in diagnosis of spinal metastases. While current practices use conventional MRI, PET-CT, and biopsies, perfusion parameters measured by DCE-MRI provide further qualitative and quantitative evidence in supporting diagnoses. DCE-MRI's detection of spinal metastases may decrease the need for radiotracer-based imaging, effectively reducing cost and patient radiation exposure.

Health Systems, Quality & Safety

Self-requested Mammography: Utilization Trends At An Academic Institution

Julia Liu, BS[1], Katherine Cavallo Hom, MD[1]
[1]Oregon Health & Science University

Introduction:

Self-requested mammograms allow eligible patients to undergo breast cancer screening without requiring an order from a referring provider. This study investigates utilization of self-requested screening and subsequent true positive rates within provider-referred and self-requested patients.

Methods:

This retrospective review analyzed screening mammograms performed at our academic institution between 2020 and 2023 (N=33,500). True positive (TP) results, defined as a diagnosis of breast malignancy within 365 days of screening, were calculated. These cases were then categorized as provider-referred or self-requested. Local availability of self-requested screening mammography was assessed (N=5).

Results:

Of 33,500 total screening mammograms, 18,947 (56.6%) were self-requested. The total number of screening mammograms steadily increased from 6,151 to 10,358 per year throughout the study period, while the percentage of self-requested mammograms also notably increased from 53.1% in 2020 to 59.4% in 2023. There were 236 TP screening mammograms, of which 117 (49.6%) were provider-referred and 119 (50.4%) were self-requested. Locally, 40% of institutions offer self-requested screening mammography for patients meeting ACR screening guidelines, without requiring additional criteria.

Discussion:

The raw number and percentage of self-requested screening mammograms demonstrate a consistent upward trend. Approximately half of all screening-detected breast malignancies originated from a self-requested mammogram by the patient. This pathway for patient access to screening mammograms is critical for early detection of breast cancer.

Conclusion:

Self-requested screening mammography usage continues to rise, which improves access to preventive screening by reducing scheduling barriers. 50.4% of all cancers found during the study period originated from self-requested screening mammography. This pathway model highlights an opportunity to improve access to patient care, as only 40% of local institutions currently offer this option without additional criteria.

Enhancing Patient Safety in Interventional Radiology: Advances in Radiation Dose Optimization

Motaz Daraghma, MD[1], Qays Abu-Saymeh, BS[2], Josh Cornman-Homonoff, MD[3], Aliaksei Salei, MD[4], Osman Ahmed, MD[5], Junaid Raja, MD[4]
[1]University of Missouri-Kansas City, Kansas City, MO
[2]University of Kansas School of Medicine-Kansas City, Kansas City, KS
[3]Yale University School of Medicine, New Haven, CT, Division of Interventional Radiology
[4]University of Alabama Birmingham, Birmingham, AL, Division of Interventional Radiology
[5]University of Chicago, Chicago, IL, Division of Interventional Radiology

Introduction:

Interventional radiology (IR) provides minimally invasive procedures that improve diagnostics, therapy, and recovery. However, these procedures often involve ionizing radiation, requiring careful dose management to ensure patient safety and optimize outcomes. Risks include skin injuries, cataracts, and long-term cancer, particularly in vulnerable groups like pediatric and pregnant patients. Recent technological advancements are transforming radiation safety in IR. Clinicians now leverage artificial intelligence (AI), real-time radiation monitoring, and improved imaging hardware to reduce dose while preserving image quality. Quality improvement measures—such as adherence to the ALARA (As Low As Reasonably Achievable) principle, implementation of Diagnostic Reference Levels (DRLs), and standardized procedural protocols—further enhance safety. Continued research and regulatory oversight are vital due to the evolving nature of IR technology. Collaboration among radiologists, physicists, technologists, and governing bodies is essential to minimize radiation risks. This review outlines key challenges and innovations in IR radiation dose management, offering strategies to improve patient outcomes through evidence-based practices.

Methods/Materials:

A comprehensive review of recent peer-reviewed studies (2018-2024) in dose optimization technologies was conducted. Key focus areas included low-dose imaging techniques, AI-enhanced dose management tools, real-time monitoring systems, and patient-specific protocols. The effectiveness of quality improvement initiatives, such as diagnostic reference levels (DRLs), ALARA principles, and standardized training programs for healthcare personnel was also assessed.

Results:

Technologies, including low dose computerized tomography (LDCT) with its iterative reconstruction algorithms and photon-counting CT (PCD-CT), reduced radiation doses without compromising diagnostic precision during interventions such as ablations. AI-powered dose-monitoring and noise-mitigation solutions further enhance real-time dose control. DRLs, routine dose audits, ALARA compliance and more have shown 20–25% dose reduction in normal imaging. The patient-specific protocols (especially in the pediatrics and oncology groups) have lowered total radiation exposure.

Conclusions:

Advances in imaging technologies, AI-powered tools and standardized protocols have improved radiation safety in IR. However, there remain challenges, including DRLs' regional differences and protocols to tailor them to. A new generation of technologies, such as AI-based dose-optimization, automated dose-tracking and spectral imaging, could still reduce dose without compromising diagnostic precision. A collaborative approach with physicists, engineers, computer scientists and physicians is needed to advance patient-centered care and make interventional radiology safer.

Injury Patterns and Imaging Utilization in Intimate Partner Violence Survivors with Limited English Proficiency

Emily Y. Yang[1,2], Alexander Kwon[1], Krishna Patel, MPH[3], Bernard Rosner, PhD[3,4], Irene Dixe de Oliveira Santo, MD[5], Bharti Khurana MD, MBA[1,6,7]
[1]Trauma Imaging Research and Innovation Center, Brigham and Women's Hospital
[2]Harvard Medical School
[3]Department of Biostatistics, Harvard T.H. Chan School of Public Health, Harvard University
[4]Channing Division of Network Medicine, Department of Medicine, Brigham and Women's Hospital
[5]Department of Radiology, Yale School of Medicine
[6]Founder and Director, Trauma Imaging Research and Innovation Center, Brigham and Women's Hospital
[7]Associate Professor of Radiology at Harvard Medical School

Rationale and Objectives:

Intimate partner violence (IPV) has a disproportionate impact on minority and underserved populations due to sociocultural barriers in help-seeking and healthcare access. We argue that language fluency forms a central component of such barriers and thus seek to explore the relationship between IPV and English language proficiency in radiologically evident injury patterns and imaging utilization.

Materials and Methods:

Dataset consisted of women ≥18 years old reporting IPV to Brigham and Women's Hospital from 2013–2018 (IPV+; n=1451), with 1-to-6 matching from our patient registry to build the controls (IPV-; n=6679). Using the patients' primary language from their medical records, we formed four groups: IPV+Non-English-Speaking (NES), IPV+English-Speaking (ES), IPV-NES, and IPV-ES. We estimated injury incidence rate ratios (IRRs) with Poisson regression and used logistic regression to assess injury odds and imaging utilization based on IPV and English proficiency. Categorical data was analyzed using the chi-square test. All statistical analyses were conducted with a significance level of $p < 0.05$ using R or MATLAB.

Results:

We observed significant differences in injury distribution by anatomic area, type, and severity across all four groups ($p<0.001$). However, English proficiency alone did not have a significant effect on IRRs by anatomic area or severity level. IPV was identified at a later age in NES vs. ES patients (44.25 vs. 38.64 years). All IPV+ patients received increased imaging studies, but English proficiency alone did not have a significant effect on imaging utilization.

Conclusion:

English language proficiency alone does not significantly affect the injury frequency, severity level, or imaging utilization in IPV survivors.

Association of Race with Bone Attenuation Loss: A Longitudinal Interaction Term Analysis with Vitamin D Status Using the Multi-Ethnic Study of Atherosclerosis

Roham Hadidchi, BS[1,2], Elena Ghotbi, MD[2], Quincy A. Hathaway, MD, PhD[3], Michael P. Bancks, PhD, MPH[4], David A. Bluemke, MD, PhD, MsB[5], R. Graham Barr, MD, DrPH[6], Wendy S. Post, MD, MS[7], Matthew Budoff, MD[8], Joao A.C. Lima, MD[7], Shadpour Demehri, MD[2]
[1]Nova Southeastern University Dr. Kiran C. Patel College of Osteopathic Medicine
[2]Russell H. Morgan Department of Radiology and Radiological Science, Johns Hopkins Medicine
[3]Department of Radiology, University of Pennsylvania
[4]Wake Forest University School of Medicine
[5]Department of Radiology, University of Wisconsin School of Medicine and Public Health
[6]Department of Medicine, Columbia University Medical Center
[7]Division of Cardiology, Department of Medicine, Johns Hopkins University School of Medicine
[8]Lundquist Institute at Harbor-University of California Los Angeles School of Medicine

Introduction:

Vitamin D deficiency is associated with increased risk of bone loss and subsequent increased risk of osteoporosis and associated complications. White individuals are known to experience more accelerated bone loss than Black individuals. No prior studies have investigated the interaction between race and vitamin D status longitudinally for bone health assessment.

Methods:

Using data from the Multi-Ethnic Study of Atherosclerosis (MESA), we selected Black and White participants with non-contrast chest CT taken at Exam 5 and Exam 6 (n=756). We used our previously developed deep learning (DL) algorithm to automatically segment the thoracic vertebrae and used the Hounsfield units (HU) of the trabecular bone to calculate volumetric BMD at each vertebral level (T1–T10) using a previously validated phantom calibration (Figure 1). To calculate change in BMD over time, we computed the annual change in BMD (mg/cm^3/year) for each participant between Exam 5 and 6. Linear regression models were used to investigate changes in BMD with respect to race (Black vs White) and season-adjusted serum vitamin D deficiency status (<25 ng/mL). Models were adjusted for baseline age, sex, body mass index, use of medications (glucocorticoids, bisphosphonates, raloxifene, calcitonin), current alcohol consumption, diabetes, serum calcium and parathyroid hormone, and Exam 5 and 6 scanner type.

Results:

Among MESA participants, 311 Black and 433 White individuals met inclusion criteria, with a median of 6.33 years between the two non-contrast chest CT scans. In the model using participants from all three included races, vitamin D deficiency status was not associated with BMD changes (β = –0.10 [–0.62, 0.41], p=0.69). Being White (as opposed to Black) was associated with a faster decline in BMD by 0.62 mg/cm^3/year (β = –0.62 [–1.10, –0.13], p=0.013). We used an interaction term between vitamin D deficiency status and race and found a significant association (p=0.050),

prompting analyses stratified by baseline vitamin D status. The association between race and BMD loss was significant only among participants who were vitamin D deficient at baseline (β = –0.69 [–1.19, –0.19], p=0.0072), and not in those normal vitamin D levels (β = –0.51 [–1.11, 0.09], p = 0.096) (Table 1).

Discussion:

Our observational study is the first to longitudinally investigate the interaction between race and vitamin D deficiency status in association with BMD loss over more than 6 years of follow-up.

Conclusion:

Only in vitamin D deficient MESA participants, White race is associated with longitudinal bone loss as compared to Black race. Our observational results suggest diligent vitamin D supplementation could alleviate the widely accepted vulnerability of White vs. Black individuals for accelerated bone loss, which can be verified in future randomized clinical trials.

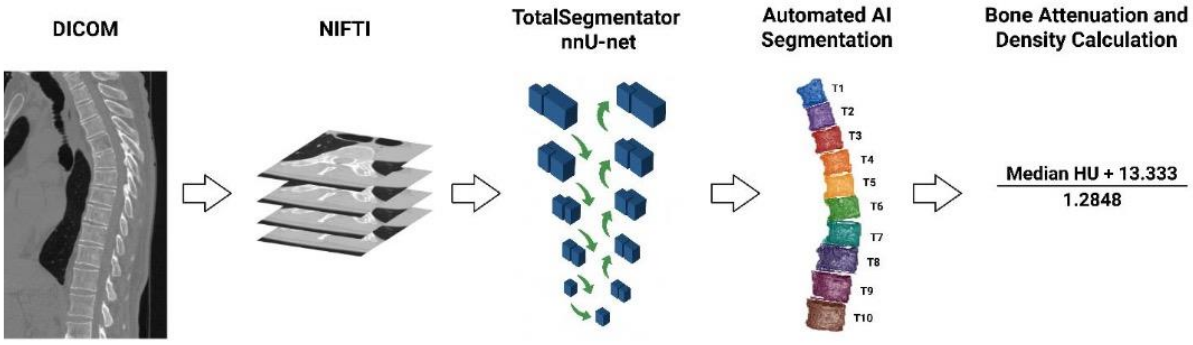

Figure 1. Workflow for deep learning-based segmentation of thoracic vertebrae on chest CT and extraction of bone mineral density.

Subgroup	Exam 5 BMD [IQR]	Exam 6 BMD [IQR]	Estimated difference in BMD change (mg/cm^3)/year [95% CI]	*p* for interaction
All participants (n=756)				
Black (n=320)	217.23 [191.59, 246.95]	219.13, [190.33, 254.70]	Reference	
White (n=436)	178.16 [156.27, 200.75]	176.82 [153.58, 204.28]	β = –0.62 [–1.10, –0.13], ***p*=0.013**	
Participants with vitamin D deficiency (n=393)				
Black (n=242)	220.96 [196.65, 253.33]	224.42 [192.84, 259.72]	Reference	**0.050**
White (n=151)	178.55 [154.30, 201.24]	176.47 [148.80, 207.02]	β = –0.69 [–1.19, –0.19], ***p*=0.0072**	
Participants without vitamin D deficiency (n=363)				
Black (n=78)	203.88 [180.61, 230.25]	204.82 [178.48, 230.37]	Reference	
White (n=285)	177.38 [157.92, 199.72]	177.41 [155.85, 202.55]	β = –0.51 [–1.11, 0.09], *p*=0.096	

Table 1. Longitudinal changes in vertebral bone mineral density (BMD) with respect to participant race and vitamin D deficiency status. Linear regression models compared rate of change in BMD per year, adjusting for baseline age, sex, body mass index, use of medications (glucocorticoids, bisphosphonates, raloxifene, calcitonin), current alcohol consumption, diabetes, serum calcium and parathyroid hormone, and Exam 5 and 6 scanner type. BMD, bone mineral density. IQR, inter-quartile range. CI, confidence interval.

Evaluating the Quality of Systematic Review Search Methodologies in Top Radiology Journals

Kinan Sawar, BS[1]
[1]Wayne State University School of Medicine

Introduction:

Systematic reviews of high-quality primary studies are considered the highest level of evidence in medicine.[1] The quality of systematic reviews depends highly on the comprehensiveness of the included literature and the reproducibility of the systematic review's search strategy.[2] A 16-item list of criteria called the Preferred Reporting Items for Systematic Reviews and Meta-Analyses literature search extension (PRISMA-S) was created in 2021 by an international research collaborative to provide guidelines regarding the reporting of search methodologies in systematic reviews. A guideline like this was necessary to standardize search-methodology reporting practices so that future systematic reviews could be reproducible. A recent study revealed that fewer than 5% of systematic reviews indexed in PubMed that were randomly sampled in November 2021 provided enough information for all database searches to be reproduced.[3] Moreover, only 1% of those reviews met six key PRISMA-S items of the total 16 items. No study has quantified PRISMA-S adherence in high-impact radiology journals.

Methods:

Using PubMed, we took a simple random sample of 50 systematic reviews from each of the three highest impact factor radiology journals (*Radiology, European Radiology,* and the *American Journal of Roentgenology*) from May 2022 to April 2025. For every systematic review, we extracted the journal name, publication year, presence of a librarian or information specialist co-author, systematic review protocol registration status (e.g., PROSPERO or Open Science Framework registries), and documentation of whether each of the six key PRISMA-S elements—search strategy name, multi-database searching, full search strategy, limits/restrictions, search dates, and total records—were reported within the review. The primary outcome was the proportion of systematic reviews reporting all six PRISMA-S items. Secondary analyses quantified the proportion of systematic reviews reporting each individual PRISMA-S item and identified publication variables associated with higher PRISMA-S adherence.

Results:

Among 75 systematic reviews sampled from *Radiology, European Radiology*, and *American Journal of Roentgenology*, only 12% reported all six key PRISMA-S search elements with no difference in PRISMA-S compliance between journals ($p = 0.56$). Item-level compliance was highest for reporting search dates (92%) and database names (80%), followed by limits/restrictions (50%), multi-database searching (65%), total records retrieved (40%), and reproduction of the full search strategy (35%). Reviews co-authored by a librarian or information specialist were over three times more likely to report all six key PRISMA-S (OR = 3.6, 95% CI: 1.1-11.5).

Discussion:

Poorly reported search strategies hinder systematic review reproducibility, limit an editorial team's ability to assess the comprehensiveness of search methodologies, and may result in missed studies that alter conclusions and ultimately misguide clinical decisions. By benchmarking PRISMA-S adherence in leading radiology journals, this study helped identify search reporting deficiencies and will help promote editorial policy modification so that submitted systematic reviews are evaluated against PRISMA-S criteria.

Conclusion:

If radiology journals adopt more stringent standards for assessing systematic-review search methodologies, future reviews will yield more reliable findings and enhanced reproducibility.

References:

1. Reddy AK, Scott J, Checketts JX, et al. Levels of evidence backing the AAOS clinical practice guidelines. Journal of Orthopaedics, Trauma and Rehabilitation. 0(0):2210491721992533. doi:10.1177/2210491721992533
2. Cooper H, Hedges LV, Valentine JC. The handbook of research synthesis and meta-analysis. Russell Sage Foundation; 2019.
3. Rethlefsen ML, Brigham TJ, Price C, et al. Systematic review search strategies are poorly reported and not reproducible: a cross-sectional metaresearch study. Journal of Clinical Epidemiology. 2024;166doi:10.1016/j.jclinepi.2023.111229

Case Reports

The Radiographic Features of Post-Polio Syndrome

Yasmine Kasiri, BS[1], Ryan Uchimura, DO[2]
[1]Western University of Health Sciences
[2]Riverside University Health System

Introduction:

Poliomyelitis, caused by the largely curtailed poliovirus, is a disease that affects the anterior horn of the spinal cord, resulting in motor neuron destruction that leads to profound hemi-atrophy of the bones and muscles. Post-poliomyelitis syndrome (PPS) is a sequela of the initial disease that occurs 15–40 years after infection, causing new onset neuromuscular weakness in the previously affected limbs. This case illustrates the radiographic manifestations of PPS, which can cause striking musculoskeletal atrophy.

Case Description:

A 59 year old female with a medical history significant for childhood polio presented with four months of increased fatigue and weakness, new paresthesias, and worsening atrophy of her left lower extremity. Physical examination revealed 2/5 left lower extremity (LLE) weakness and significant atrophy of multiple lower extremity muscle groups. Imaging showed asymmetric osteopenia of the left hemipelvis and femur. CT of the abdomen and pelvis revealed severe muscular fatty atrophy of the left iliopsoas, gluteus muscles, and thigh muscles.

Discussion:

Poliomyelitis is a neuromuscular disease that results due to infection from poliovirus which damages the ventral horn motor neurons. Although the transmission of poliovirus has largely been prevented since the widespread implementation of the polio vaccine, childhood survivors continue to experience the long-term effects of PPS. PPS is a progressive, incurable condition that emerges decades after acute infection in 25–40% of affected individuals. The syndrome is theorized to arise from abnormal motor unit enlargement following axonal sprouting in response to anterior horn cell loss during acute poliomyelitis, eventually rendering these reinnervated units metabolically unsustainable. Contributing factors such as overuse, aging, and persistent inflammation—with a role for reactivated poliovirus or an autoimmune process—may further accelerate motor unit failure and functional decline.

PPS is a clinical diagnosis of exclusion supported by a history of prior poliomyelitis, a period of recovery and stable neuromuscular function, and the gradual onset of new, progressive muscle weakness or fatigue that persists for one year. PPS is typically not life-threatening and slowly progressive, as it impacts mobility and quality of life, often requiring long-term supportive care.

Radiographic manifestations of PPS can be attributed to the destruction of motor neurons with resultant unilateral limb atrophy, joint pain, and paresthesias. In the acute phase, poliomyelitis is typically not radiographically evident but findings may include T2 hyperintensity on MRI involving the anterior horns due to gliosis and edema, which progresses to cord atrophy in later

stages. Chronically, PPS causes denervation with subsequent fatty atrophy of the affected muscle groups which leads to disuse osteopenia manifesting as decreased osseous cortical thickness. Marked decrease in bone mineral density and muscle bulk can cause abnormal contracture of the hip into flexion, abduction, and external rotation, a common manifestation of neuromuscular disorders.

Despite these prominent findings, it is crucial to recognize that these radiographic features are nonspecific and can overlap with other neuromuscular diseases such as ALS and Duchenne muscular dystrophy. Correlating the patient's clinical history with imaging findings aids in better understanding PPS by visually highlighting how its progressive symptoms reflect the chronic sequelae of anterior horn cell degeneration.

Renal Melanoma: Differentiating the Rare Malignancy from Common Renal Tumors Radiographically

Yasmine Kasiri, BS[1], Raymond Huang, MD[2], Monika Kief-Garcia, MD[2]
[1]Western University of Health Sciences
[2]Riverside University Health System

Introduction:

Primary melanoma of the kidney is an exceptionally rare presentation of renal malignancy with only a handful of cases reported in the literature. The most common renal cancer is renal cell carcinoma (RCC), which comprises 95% of malignant renal tumors, with subtype clear cell renal carcinoma accounting for 75% of these cases, followed by papillary RCC accounting for 10–15% of cases, and with renal sarcomas proving to be especially uncommon, constituting less than 1% of renal malignancies. In this report, we will highlight the distinctive radiographic characteristics of this rare renal melanoma and discuss how they aid in differentiating it from more common renal malignancies.

Case Descriptions:

We present the case of a 78-year-old female with no known family history of cancer who presented with a one-month history of left-sided abdominal pain radiating to the flank and an unintentional weight loss of 20 pounds. Physical examination revealed an appreciable left upper quadrant mass with associated tenderness. Initial imaging, including contrast-enhanced computed tomography and magnetic resonance imaging, demonstrated a large, heterogeneously enhancing soft tissue mass measuring 18.5 x 14 x 15.5 cm, arising from the left kidney with mass effect on surrounding structures. The patient underwent an extensive surgical resection, including left nephrectomy, en bloc colectomy, subtotal pancreatectomy, and splenectomy. Follow up PET scan showed no evidence of metastatic disease, and genomic testing of the specimen indicated an 89% probability of melanoma. Given the rarity of renal melanoma and the lack of established treatment guidelines, the case continues to be reviewed at the multidisciplinary tumor board.

Discussion:

The radiographic features of the different primary renal tumors display both distinct and overlapping characteristics, which, when analyzed alongside clinical presentation, could potentially assist in diagnosis and inform treatment decisions. By characterizing the imaging features of this rare case of primary renal melanoma, we can contribute insights regarding the clinical features of this remarkable presentation to the literature. Furthermore, by extrapolating from what is known about the imaging characteristics of more common renal tumors, we can enhance our understanding of this rare occurrence, despite the absence of prior cases of renal melanoma.

References:

1. Uhlig J, Uhlig A, Bachanek S, Onur MR, Kinner S, Geisel D, Köhler M, Preibsch H, Puesken M, Schramm D, May M, De Visschere P, Weber MA, Surov A. Primary renal sarcomas: imaging features and discrimination from non-sarcoma renal tumors. Eur Radiol. 2022 Feb;32(2):981–989. doi: 10.1007/s00330-021-08201-4. Epub 2021 Jul 31. PMID: 34331576; PMCID: PMC8794936.
2. Keraliya AR, Krajewski KM, Braschi-Amirfarzan M, Tirumani SH, Shinagare AB, Jagannathan JP, Ramaiya NH. Extracutaneous melanomas: a primer for the radiologist. Insights Imaging. 2015 Dec;6(6):707–17. doi: 10.1007/s13244-015-0427-8. Epub 2015 Sep 3. PMID: 26334521; PMCID: PMC4656230.
3. Alevizakos M, Gaitanidis A, Korentzelos D, Basourakos SP, Burgess M. Renal Sarcoma: A Population-Based Study. Clin Genitourin Cancer. 2023 Feb;21(1):155–161. doi: 10.1016/j.clgc.2022.07.012. Epub 2022 Jul 30. PMID: 36045013; PMCID: PMC11186599.
4. Keraliya AR, Krajewski KM, Braschi-Amirfarzan M, Tirumani SH, Shinagare AB, Jagannathan JP, Ramaiya NH. Extracutaneous melanomas: a primer for the radiologist. Insights Imaging. 2015 Dec;6(6):707–17. doi: 10.1007/s13244-015-0427-8. Epub 2015 Sep 3. PMID: 26334521; PMCID: PMC4656230.

Metastatic Parathyroid Carcinoma with Refractory Hypercalcemia and Multimodal Imaging Findings: A Case Review

Arian Karimi, BHSc[1], Omair Ali, MD[2], Fang Zhu, MD, PhD[2]
[1]University of Illinois College of Medicine – Chicago Campus
[2]Department of Radiology, UI Health

Introduction:

Parathyroid carcinoma is a rare type of cancer and one of the causes of primary hyperparathyroidism (PHPT). It often presents with clinical symptoms including but not limited to hypercalcemia, neck mass, bone disease, etc. Hence, given the rarity, conditions such as parathyroid adenoma and primary parathyroid hyperplasia are often considered first on differential diagnosis. Ultimately, the diagnosis involves a multidisciplinary group of healthcare fields, from genetics and oncology to radiology and surgery specialties. The study aims to review the longitudinal imaging findings, pitfalls in imaging, the importance of nuclear medicine imaging, and multidisciplinary management of a rare case of metastatic parathyroid carcinoma.

Methods:

A 55-year-old female patient was diagnosed with parathyroid carcinoma after undergoing total thyroidectomy. Serial CT, ultrasound, sestamibi-based SPECT/CT parathyroid scans, and FDG PET/CT studies were used to evaluate disease recurrence, metastatic progression, and treatment response. Imaging findings were correlated with clinical parameters and treatments.

Results:

Initial imaging demonstrated findings suggesting a parathyroid adenoma and thyroid nodule with FNA cellular analysis suggesting a thyroid malignancy. Surgical pathology indicated parathyroid carcinoma. Post-thyroidectomy surveillance imaging (2019–2021) showed no recurrence. In 2022, CT and PET identified multiple pulmonary nodules and a neck lesion, with subsequent growth and new nodules observed in follow-up studies. However, serial imaging studies did not detect definitive recurrent metastatic disease.

Serial CT studies documented interval growth of treated lung nodules, and PET/CT studies revealed nonspecific hypermetabolic activity in these nodules. However, the most recent NM parathyroid SPECT/CT demonstrated increased uptake in cervical/thoracic lymph nodes and pulmonary nodules, indicating metastatic recurrent disease. Imaging findings paralleled rising PTH and hypercalcemia, underscoring the progression of metastatic activity.

Discussion:

Although there have been advancements in imaging modalities, limitations do exist. For example, adenomas share similar image features with carcinomas and thyroid lesions emphasizing the need for prompt pathological review of the specimen. In nuclear imaging, Sestamibi uptake is high in mitochondria-rich oxyphil cells while showing low-mild uptake in malignant cells making it difficult to fully ascertain the different types of cells. In FDG-PET/CT imaging, micro metastatic

lesions are easily missed, and larger nodules may not be FDG-avid. Lastly, 68-Ga-DOTATATE PET/CT imaging has limited evaluation for recurrence. As a result, it further showcases the need for a comprehensive examination including laboratory work, physical examination, imaging, and multidisciplinary expertise input when it comes to cancer surveillance.

Conclusion:

This case highlights the critical role of multimodal imaging in managing metastatic parathyroid carcinoma. It also demonstrates the complexity of evaluating treatment response, including the potential pitfalls of surveillance imaging and the importance of multidisciplinary management.

References:

1. Chakrabarty N, Mahajan A, Basu S, D'Cruz AK. Imaging Recommendations for Diagnosis and Management of Primary Parathyroid Pathologies: A Comprehensive Review. Cancers (Basel). 2024;16(14):2593. Published 2024 Jul 19. doi:10.3390/cancers16142593
2. Eldaya RW, Calle S, Wong FC, Learned KO, Wintermark M. Parathyroid carcinoma: Imaging features of initial presentation and recurrence. A single center experience. Neuroradiol J. 2024;37(1):92-106. doi:10.1177/19714009231212361
3. Guo YH, Huang JW, Wang Y, Lu R, Yang MF. Value of 99m Tc-MIBI SPECT/CT in the localization of recurrent lesions in patients with suspected recurrent parathyroid carcinoma. Nucl Med Commun. 2023;44(1):18-26. doi:10.1097/MNM.0000000000001641
4. Machado NN, Wilhelm SM. Parathyroid Cancer: A Review. Cancers (Basel). 2019;11(11):1676. Published 2019 Oct 28. doi:10.3390/cancers11111676
5. Naik M, Khan SR, Owusu D, et al. Contemporary Multimodality Imaging of Primary Hyperparathyroidism. Radiographics. 2022;42(3):841-860. doi:10.1148/rg.210170
6. Strauss SB, Roytman M, Phillips CD. Parathyroid Imaging: Four-dimensional Computed Tomography, Sestamibi, and Ultrasonography. Neuroimaging Clin N Am. 2021;31(3):379-395. doi:10.1016/j.nic.2021.04.007

NICE Lesions and Aneurysm Repair: Expanding Awareness of a Rare Complication

Jacob Devine, BS[1], Alexander Withrow, BS[1], Andrew Holmes, MD[1], Tanner Redlin, MD[1], Megan Albertson, MD[1]
[1]University of South Dakota Sanford School of Medicine

Abstract:

Non-ischemic cerebral enhancing (NICE) lesions are a rare complication among the potential complications of aneurysmal repair. NICE lesions are believed to arise from migrated embolic materials and continue to cause diagnostic challenges due to their delayed onset, non-specific clinical symptoms, and comparable imaging findings to other more common conditions. This article discusses the pathophysiology, clinical presentation, imaging characteristics, differential diagnosis, and management strategies of NICE lesions, highlighting the characteristic imaging findings and relevant clinical features which are used to establish a clinical diagnosis and provide expedited treatment. In addition, this article aims to improve recognition of NICE lesions, identify risk factors, recognize their clinical impacts in order to improve patient outcomes following endovascular procedures.

Conclusion:

NICE lesions are a rare but important complication of neurovascular aneurysm repair. Identifying NICE lesions remains challenging due to the absence of routine follow-up MRI and the resemblance to more common complications. Key imaging features include a waxing and waning pattern on follow-up exams and confinement to the vascular territory corresponding to the site of endovascular intervention. Radiologists who are familiar with rare complications of aneurysm repair, such as NICE lesions, are more likely to describe them in the differential and create appropriate treatment plans for patients.

References:

1. Armoiry X, Turjman F, Hartmann DJ, et al. Endovascular Treatment of Intracranial Aneurysms with the WEB Device: A Systematic Review of Clinical Outcomes. *AJNR Am J Neuroradiol.* 2016;37(5):868-872. doi:10.3174/ajnr.A4611
2. Bayas A, Christ M, Berlis A, et al. Incidence, clinical spectrum, and immunotherapy of non-ischemic cerebral enhancing lesions after endovascular therapy. *Ther Adv Neurol Disord.* 2022;15:17562864211072372.Published 2022 Jan 31. doi:10.1177/17562864211072372
3. Cai Y, Huang L, Hao J, Xie F, Ling T, Richard SA. Delayed Multiple Non-ischemic Cerebral Enhanced Lesions After Endovascular Therapy For Left Internal Carotid Aneurysm: A Case Report. *Curr Med Imaging.* 2021;17(8):1031-1035. doi:10.2174/1573405617666210122085247
4. Forestier G, Escalard S, Sedat J, et al. Non-ischemic cerebral enhancing lesions after thrombectomy: a multicentric retrospective French national registry. *Neuroradiology.* 2022;64(5):1037-1042. doi:10.1007/s00234-022-02919-8

5. Gaillard F, Sharma R, Botz B, Non-ischemic cerebral enhancing (NICE) lesions. Reference article, *Radiopaedia.org* (Accessed on 11 Oct 2024) https://doi.org/10.53347/rID-151711
6. Guetarni Z, Bernard R, Boulouis G, et al. Longitudinal radiological follow-up of individual level non-ischemic cerebral enhancing lesions following endovascular aneurysm treatment. *J Neurointerv Surg.* 2024;16(8):838-845. Published 2024 Jul 16. doi:10.1136/jnis-2023-020060
7. Ihn YK, Shin SH, Baik SK, Choi IS. Complications of endovascular treatment for intracranial aneurysms: Management and prevention. *Interv Neuroradiol.* 2018;24(3):237-245. doi:10.1177/1591019918758493
8. Javed K, Fortunel A, Holland R, et al. Identifying risk factors for perioperative thromboembolic complications in patients treated with the Woven EndoBridge device. *Interv Neuroradiol.* 2023;29(5):561-569. doi:10.1177/15910199221113907
9. Mantilla DE, D Vera D, Ortiz AF, Nicoud F, Costalat V. The Woven EndoBridge device, an effective and safe alternative endovascular treatment of intracranial aneurysm-systematic review. *Interv Neuroradiol.* Published online September 11, 2023. doi:10.1177/15910199231201544
10. Mouchouris N, Hasan D, Samaniego EA, et al. The Woven EndoBridge (WEB) device: feasibility, techniques, and outcomes after FDA approval. *J Neurosurg.* 2021;136(5):1266-1272. Published 2021 Oct 8. doi:10.3171/2021.5.JNS21889
11. Moughal S, Booth TC. Correspondence on 'Non-ischemic cerebral enhancing (NICE) lesions after flow diversion for intracranial aneurysms: a multicenter study' by Richter et al. *J Neurointerv Surg.* Published online February 22, 2024. doi:10.1136/jnis-2024-021548
12. Pierot L, Moret J, Turjman F, et al. WEB Treatment of Intracranial Aneurysms: Feasibility, Complications, and 1-Month Safety Results with the WEB DL and WEB SL/SLS in the French Observatory. *AJNR Am J Neuroradiol.* 2015;36(5):922-927. doi:10.3174/ajnr.A4230
13. Pierot L, Barbe C, Nguyen HA, et al. Intraoperative Complications of Endovascular Treatment of Intracranial Aneurysms with Coiling or Balloon-assisted Coiling in a Prospective Multicenter Cohort of 1088 Participants: Analysis of Recanalization after Endovascular Treatment of Intracranial Aneurysm (ARETA) Study [published correction appears in Radiology. 2020 Aug;296(2):E130-E133. doi: 10.1148/radiol.2020204013.]. *Radiology.* 2020;295(2):381-389. doi:10.1148/radiol.2020191842
14. Richter C, Möhlenbruch MA, Vollherbst DF, et al. Non-ischemic cerebral enhancing (NICE) lesions after flow diversion for intracranial aneurysms: a multicenter study. *J Neurointerv Surg.* 2024;16(11):1174-1180. Published 2024 Oct 14. doi:10.1136/jnis-2023-021176
15. Santhumayar BA, White TG, Werner C, Shah K, Woo HH. Woven EndoBridge Device Migration and Microsnare Retrieval Strategy: Single Institutional Case Reports with Technical Video Demonstration. *Neurointervention.* 2023;18(2):129-134. doi:10.5469/neuroint.2023.00136
16. Shotar E, Law-Ye B, Baronner-Chauvet F, et al. Non-ischemic cerebral enhancing lesions secondary to endovascular aneurysm therapy: nickel allergy or foreign body reaction? Case series and review of the literature. *Neuroradiology.* 2016;58(9):877-885. doi:10.1007/s00234-016-1699-5

17. Shotar E, Labeyrie MA, Biondi A, et al. Non-ischemic cerebral enhancing lesions after intracranial aneurysm endovascular repair: a retrospective French national registry. *J Neurointerv Surg.* 2022;14(9):925-930. doi:10.1136/neurintsurg-2021-017992
18. Villamizar AB, Estévez MF, Vargas O, et al. A multicenter study of the efficacy and safety of treatments (endovascular or conservative) in small intracranial aneurysms in Colombia. *Interv Neuroradiol.* Published online May 15, 2024. doi:10.1177/1591019924125438

Imaging and Coil Embolization of Gastric Varices in Patient with Situs Ambiguus

Yutong Liang, BS[1], Zainab Ayoub, MD[2,3], Shane Newberger, MD[2]
[1]Michigan State University College of Osteopathic Medicine
[2]DMC/Wayne State University School of Medicine, Department of Radiology
[3]University of Utah School of Medicine, Department of Radiology

Introduction:

Situs ambiguus, also known as heterotaxy, is a rare congenital disorder characterized by abnormal arrangement of thoracoabdominal organs, often accompanied by vascular anomalies. Gastric varices (GV) are a potentially life-threatening complication of portal hypertension, often managed via endoscopic therapies or interventional procedures such as transjugular intrahepatic portosystemic shunt (TIPS) or balloon-occluded retrograde transvenous obliteration (BRTO). However, complex anatomical variants like situs ambiguus can pose unique diagnostic and therapeutic challenges. This case highlights the diagnostic intricacies and tailored interventional approach in managing GV in a patient with situs ambiguus.

Methods:

A 48-year-old male with a history of GV, type 2 diabetes, and seizure disorder presented to the ED with acute hematemesis and hemoglobin of 5.7 g/dL. He was hemodynamically stable on presentation. Physical exam was unremarkable, and prior CT imaging revealed situs ambiguus involving beaver tail liver anatomy with a right-sided spleen and tortuous splenic vasculature. After receiving three units of packed red blood cells, the patient underwent endoscopy, which identified large GV with recent stigmata of bleeding. Given his vascular anatomy and lack of a gastrorenal shunt, interventional radiology was consulted for a trans-splenic approach for coil embolization.

Results:

Ultrasound-guided trans-splenic venous access was obtained. Pre-embolization venography revealed extensive varices in the splenic hilum and stomach draining into the portal system, with preserved hepatopetal flow and no evidence of a gastrorenal shunt. Coil embolization was performed using Penumbra Ruby and Tornado coils with adjunctive gelfoam pledgets. Post-procedural venography demonstrated successful obliteration of the varices. Postoperative imaging confirmed no active bleeding, and the patient's hemoglobin stabilized at 7.2 g/dL prior to discharge. At 6-month follow-up, hemoglobin was 14.8 g/dL with no recurrence of bleeding symptoms.

Discussion:

This case underscores the importance of adapting interventional strategies to anatomical variations. The absence of portosystemic shunting and unusual organ arrangement precluded the use of TIPS or BRTO. A trans-splenic approach provided direct access to the target vasculature, allowing safe and effective coil embolization. Situs ambiguus, although rare, should be considered

in patients with unexplained or complex presentations, especially when conventional vascular access is unfeasible.

Conclusion:

In patients with situs ambiguus and GV, conventional interventions may be limited by anatomic constraints. Trans-splenic coil embolization offers a safe and effective alternative when standard approaches are contraindicated. Comprehensive imaging and individualized planning are essential for successful outcomes in such complex cases.

Differentiating Demyelinating Disorders: A Case Report

Alankrit Shatadal, BS, BA[1]
[1]University of Wisconsin-Madison School of Medicine and Public Health

Acute Disseminated Encephalomyelitis (ADEM) is a rare, acute immune-mediated demyelinating disorder of the central nervous system, often triggered by viral infections and more common in the pediatric population (usually under 15 years of age). This case describes a previously healthy 24-year-old male who presented with altered mental status, paraphasic errors, ataxia, and dysphagia. A full infectious workup was negative. MRI findings of diffuse multiple non-enhancing hyperintense lesions on T2-weighted and DWI sequences, predominantly involving the subcortical white matter of bilateral hemispheres and cerebellum, were critical in differentiating ADEM from the leading clinical differential, tumefactive multiple sclerosis. The Callen MS criteria detail the differentiating radiologic findings between multiple sclerosis and ADEM in young adults, with a specificity of up to 95%. The absence of multiple periventricular lesions and T1-hypointense lesions in this case pointed the radiologic diagnosis towards ADEM. This patient's course ultimately displayed clinical and radiographic improvement after five rounds of plasmapheresis, and he required no further treatments to make a full recovery. This case underscores the importance of considering ADEM in the differential for acute encephalopathy with multifocal deficits and diffuse lesions on imaging.

Incidental Diagnosis of Pulmonary Alveolar Microlithiasis in a Patient with Cardiopulmonary Symptoms: A Radiologic Case Highlight

Pouria Vadipour[1], Elmira Taghi Zadeh, MD[2], Alhassan Alhasson, MD[2], Gulcin Altinok, MD[2]
[1]Western Michigan University Homer Stryker M.D. School of Medicine, Kalamazoo, MI
[2]Division of Radiology, Wayne State University, Detroit Medical Center, Detroit, MI

Introduction:

Pulmonary Alveolar Microlithiasis (PAM) is a rare autosomal recessive disorder of the lung parenchyma characterized by intra-alveolar accumulation of calcium phosphate microliths, resulting in progressive lung fibrosis and loss of function. This accumulation results from mutations in the *SLC34A2* gene encoding a sodium-phosphate cotransporter found in type II alveolar cells. PAM is frequently asymptomatic and often identified incidentally during imaging for unrelated conditions. We present a case of a 34-year-old male diagnosed with PAM during evaluation for chest pain and shortness of breath.

Methods:

A 34-year-old male with a history of heart failure, coronary artery disease, diabetes mellitus, hyperlipidemia, and schizophrenia presented to the emergency department with complaints of chest pain, dyspnea, and bilateral lower-extremity swelling. On examination, vital signs showed a heart rate of 113 beats/min, blood pressure of 148/87 mmHg, respiratory rate of 20 breaths/min, and oxygen saturation of 98% on room air. Physical examination revealed diminished breath sounds, nonspecific cardiac findings, and 2+ bilateral pitting edema. The patient underwent a chest X-ray and a computed tomography (CT) scan of the thorax as part of the initial workup.

Results:

Chest radiograph and CT scan revealed prominent bronchovascular markings, heterogeneous airspace disease, and numerous punctate calcifications diffusely involving the lung fields. The CT scan demonstrated clustered calcified nodules in both upper and lower lobes, producing a “sandstorm lung” appearance—typical of PAM. Subpleural sparing of the pulmonary calcifications, or the “black pleura” sign, was also noted, further supporting the diagnosis. Based on these pathognomonic findings, PAM was diagnosed incidentally. The patient received conservative management focused on supportive care alongside symptom control and was discharged with arrangements for outpatient follow-up.

Discussion:

PAM is often diagnosed incidentally due to its indolent course and nonspecific symptoms. Its hallmark radiologic findings—“sandstorm” calcifications and subpleural sparing—can be diagnostic in the appropriate clinical context. Genetic testing may confirm mutations in *SLC34A2*, but imaging alone is often sufficient for diagnosis when classic features are present. The disease typically progresses slowly but may eventually lead to restrictive lung disease and respiratory

failure. Currently, there is no curative treatment; lung transplantation remains the only definitive option in advanced cases. Early detection allows for close monitoring, symptomatic management, and patient education regarding potential disease progression.

Conclusion:

This case illustrates the importance of recognizing characteristic imaging patterns in diagnosing rare conditions such as PAM. Awareness of PAM's radiographic features allows clinicians to make timely diagnoses even in patients without overt respiratory symptoms. Early identification may improve long-term outcomes through surveillance and supportive interventions aimed at preserving lung function.

Education & Training

Recruiting the Next Generation of Radiologists: A Medical School Radiology Pipeline Template

Melis Ozkan, BS[1], Lauren L. Hoff, MD, MS[2], David A. Bloom, MD, FACR, FAAP[3], Katherine A. Klein, MD, FACR[3]
[1]University of Michigan Medical School,
[2]University of California Los Angeles Health,
[3]Department of Radiology, University of Michigan, Ann Arbor, Michigan

Purpose:

The University of Michigan Radiology Pipeline, now "RadLine," was designed to integrate medical students within the Department of Radiology. Programming includes shadowing, simulation learning, lectures, longitudinal mentorship, networking, and research opportunities. It is targeted towards first-year medical students. Programs such as this one are desired by medical students.[1] Early, accessible, and affordable exposure with role models in radiology is the first step in recruiting future radiologists who bring new perspectives to the field.[2]

The program is organized into "RadFams," groups composed of 1–2 attending radiologists, 2–3 residents/fellows, and 3–4 students. We aim to share the template for this program across institutions with the goal of increasing exposure to radiology and helping to recruit the next generation of radiologists from varying regions and backgrounds.

Methods:

First-year medical students at the University of Michigan were selected to join RadLine through an electronic application process. Medical student cohort totals included 18 (2023), 20 (2024), and 12 (2025). The first cohort (C1) is now third-years, the second cohort (C2) second-years on clinical clerkships, and the third cohort (C3) first-years. Descriptive statistics were performed on surveys collecting demographic data, perceptions of radiology, and specialty choice post-program.

Results:

The percentage of students identifying as URiM was 44% in C1, 40% in C2, and 83% in C3. The percentage identifying as female was 53% in C1, 55% in C2, and 67% in C3. Specialty choice response rate was 77% from C1 and 65% from C2. Overall, the top three specialty choices across C1 and C2 were 40.7% undecided, 14.8% Diagnostic/Interventional Radiology, and 11.1% Internal Medicine. Perceptions of radiology were 82% positive, 18% neutral, and 0% negative. Qualitatively, students choosing another specialty expressed that this was still a valuable experience but wanted more intense patient contact (37%) or invasive surgical participation (15%).

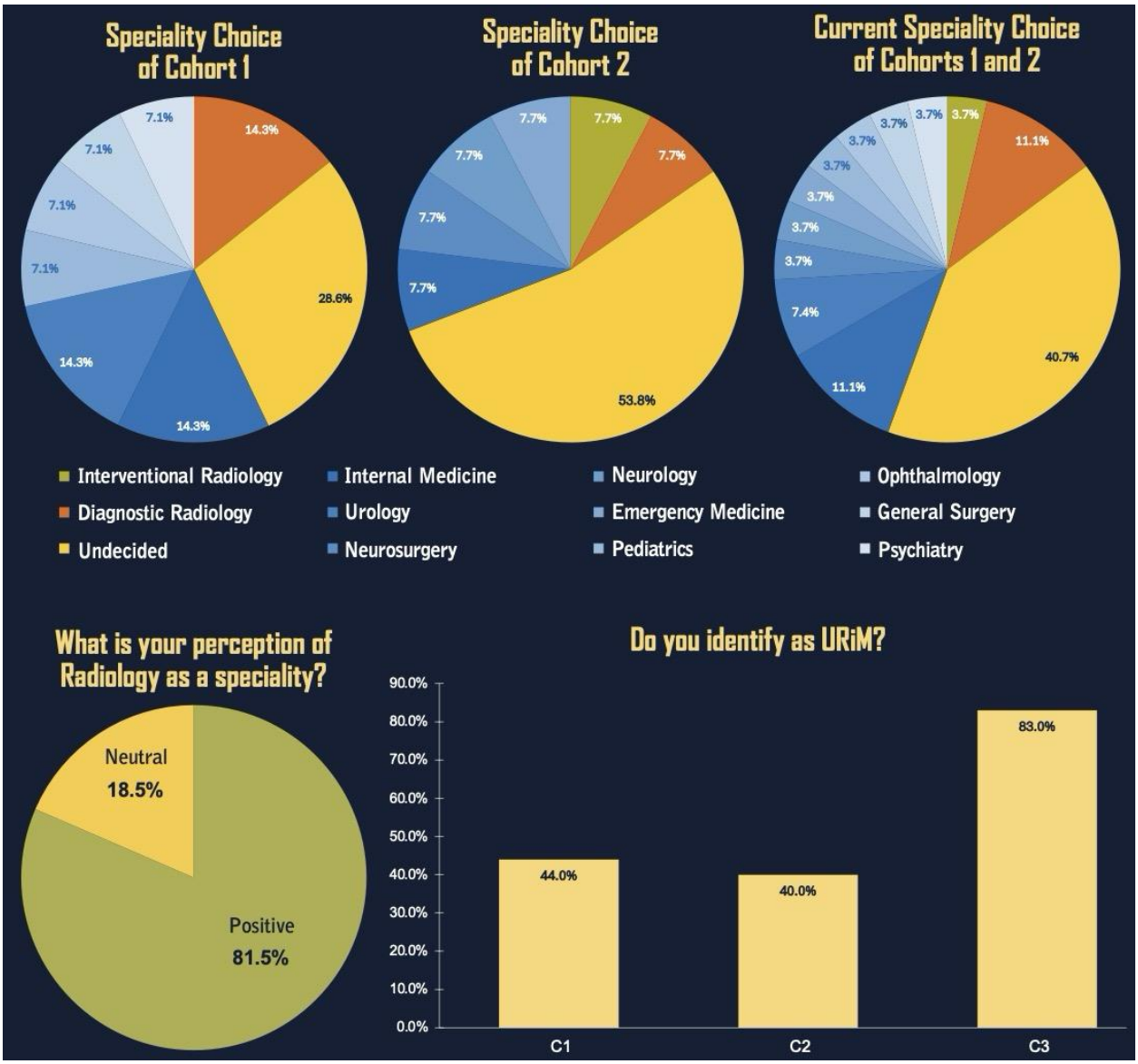

Conclusion:

The pipeline has increased understanding and interest in radiology for students, particularly those underrepresented in medicine or early in their medical education. 14.8% have subsequently declared interventional or diagnostic radiology as a career interest. Students who initially chose another specialty still reported that the pipeline positively impacted their perception of radiology. As the first radiology pipeline program designed for medical students using this framework, RadLine offers a promising model to inspire students to consider radiology starting in the preclinical years. The structured program has the potential to support early mentorship, sustained clinical exposure, and professional identity formation. With the program's scalability and success, RadLine provides a template to strengthen the pipeline into radiology, foster interest among diverse learners, and recruit the next generation of radiologists early in medical school.

References:

1. Hernandez CO, Parilla D, Turner M, Johnson MH. Mentoring the Next Generation of Radiologists: A Medical Student Radiology Pipeline Program. JACR. 2022 Dec;19(12):1737-1739. doi:10.1016/j.jacr.2022.07.014
2. Estelle SD, Eslami S, Bhargavan M, Wall D, Arleo EK, Nicola GN. Medical Student Mentoring Programs: Current Insights and Future Directions. J Am Coll Radiol. 2023 Jan;20(1):5-8. doi:10.1016/j.jacr.2022.09.004

Refining Radiology Education for Medical Undergraduates: A Student-Led, Faculty-Guided Update of a Preclinical Anatomy and Radiology Website

Trevor Canty, BA[1], Travis Byrum, MD[1], Liam Locke, MD[1], Virginia Lyons, PhD[1], Nancy McNulty, MD[1]
[1]Dartmouth Geisel School of Medicine

Introduction:

Medical students often gain limited exposure to radiology in their preclinical years compared to other disciplines of medicine. Further, many schools do not have mandatory clinical rotations in radiology during years three and four of medical school. As such, it becomes increasingly important to capitalize on the limited amount of time allotted for radiology education. Our institution's anatomy website, designed by faculty, has been used in the preclinical curriculum for years and heavily integrates radiology as a means for teaching anatomy. However, we identified that the website's interface was outdated, and it was organized by regions, which didn't match our newer, systems-based curriculum, both of which limited students' use. In addition, the method of structure labeling with dots or arrows did not encompass the full structure, which challenged students to extrapolate. Our goal was to improve the website's interface, present content in both systems based and region-based format, and to refine anatomic detail by creating anatomical borders in place of arrow labels for the thousands of pre-existing annotated scans on the website. This was a student-driven project, with students dedicated to both website design and structure labeling.

Methods:

A team of medical students interested in anatomy and radiology began the process of website redesign. A medical student with previous experience in software engineering created the structure of the new site. New features for pre-existing anatomy and radiology quizzes, which are integrated in the site, were also developed. Concomitantly, other students began mapping structures via individual point labeling via publicly available image-map.net, allowing students to finely trace the borders of anatomic structures that had previously only been labeled with arrows or dots. This process later integrated the free application Inkscape (https://inkscape.org), allowing users to trace anatomic structures with styluses on a tablet, automatically generating hundreds of coordinates. Thousands of structures were remapped and integrated into the new website. Faculty reviewed all images to ensure radiologic and anatomic accuracy, and edits were implemented, as needed. Structures with complex borders were iteratively improved, integrating both feedback from faculty as well as new imaging structures, refining anatomic detail from the original site.

Results:

A working version of the website was published and integrated into the preclinical, longitudinal anatomy and imaging curricula. Anecdotally, students reported increased ease of use as well as improved efficiency of studying structures in the institution's new systems-based curriculum. The old site was designed as single pages, with next/back buttons. The structure of the new site allows

the user to scroll continuously and easily jump from topic to topic using the table of contents in the left-hand column.

Discussion:

Implementation of student-driven improvements to a pre-existing preclinical anatomy and radiology website refined anatomic detail and user experience, allowing medical students to become uniquely involved stakeholders in their own education. Though structured evaluation is still in progress with formal surveys—a limitation of our study—informal qualitative student feedback has been positive along with positive feedback from faculty in the QI process.

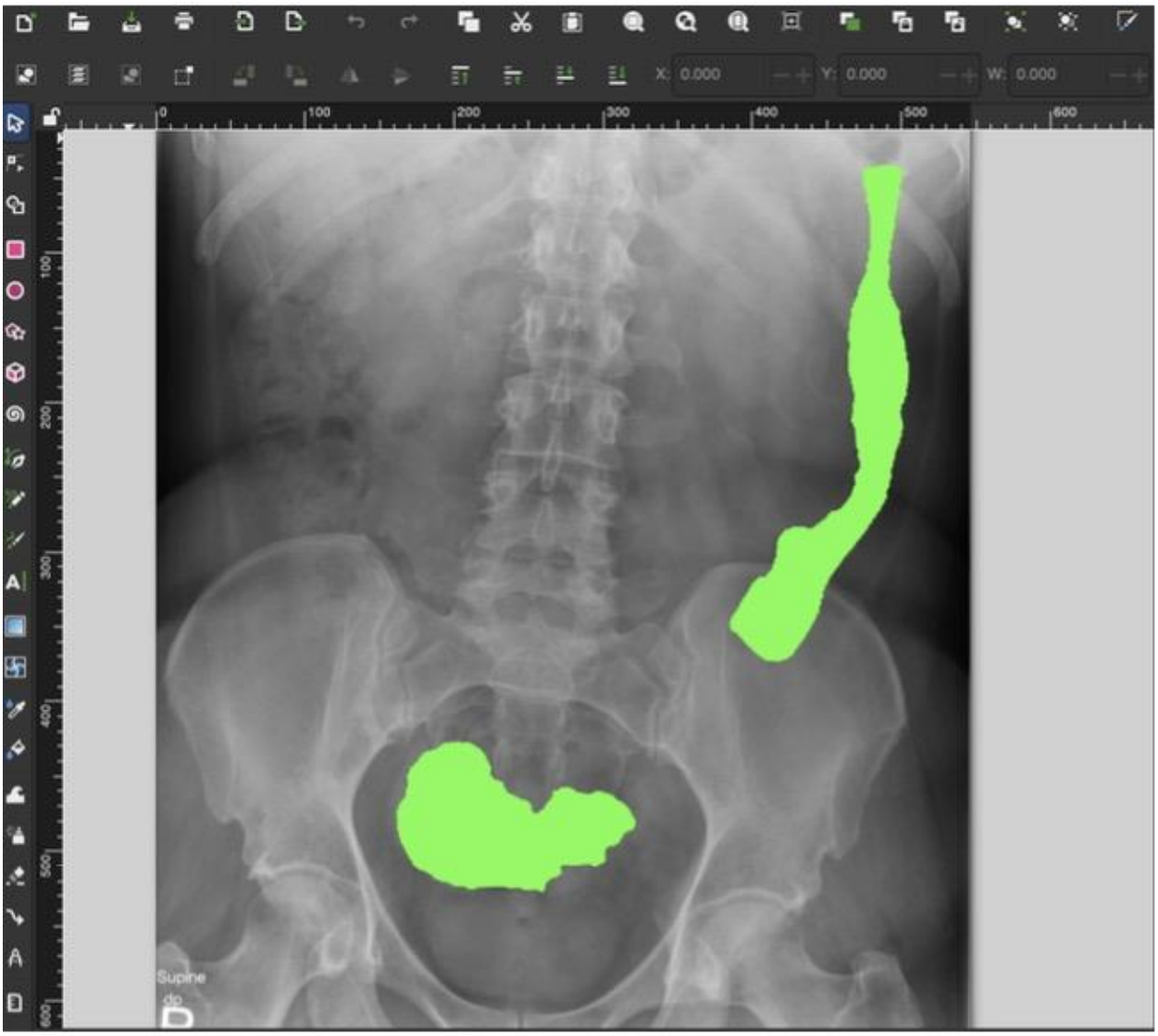

Figure 1.

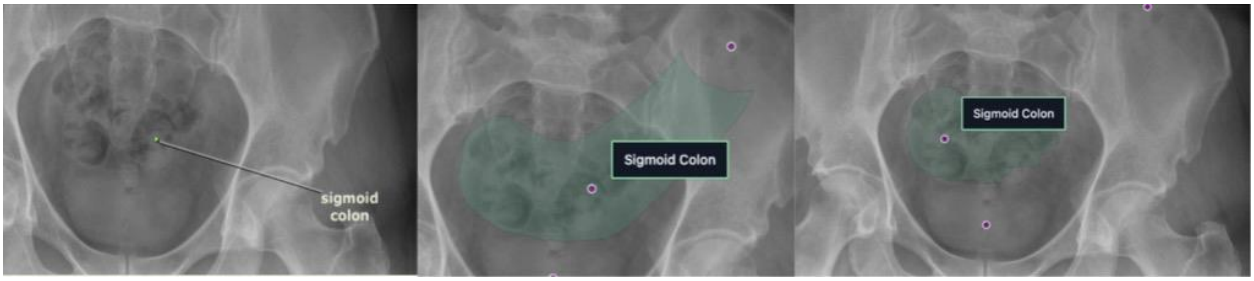

Figure 2.

Anatomic labeling evolved from the old site (left) to the new site's first mapping technique with image-map.net (middle). Finally, the addition of Inkscape allowed for hundreds of coordinates to produce smooth borders (right).

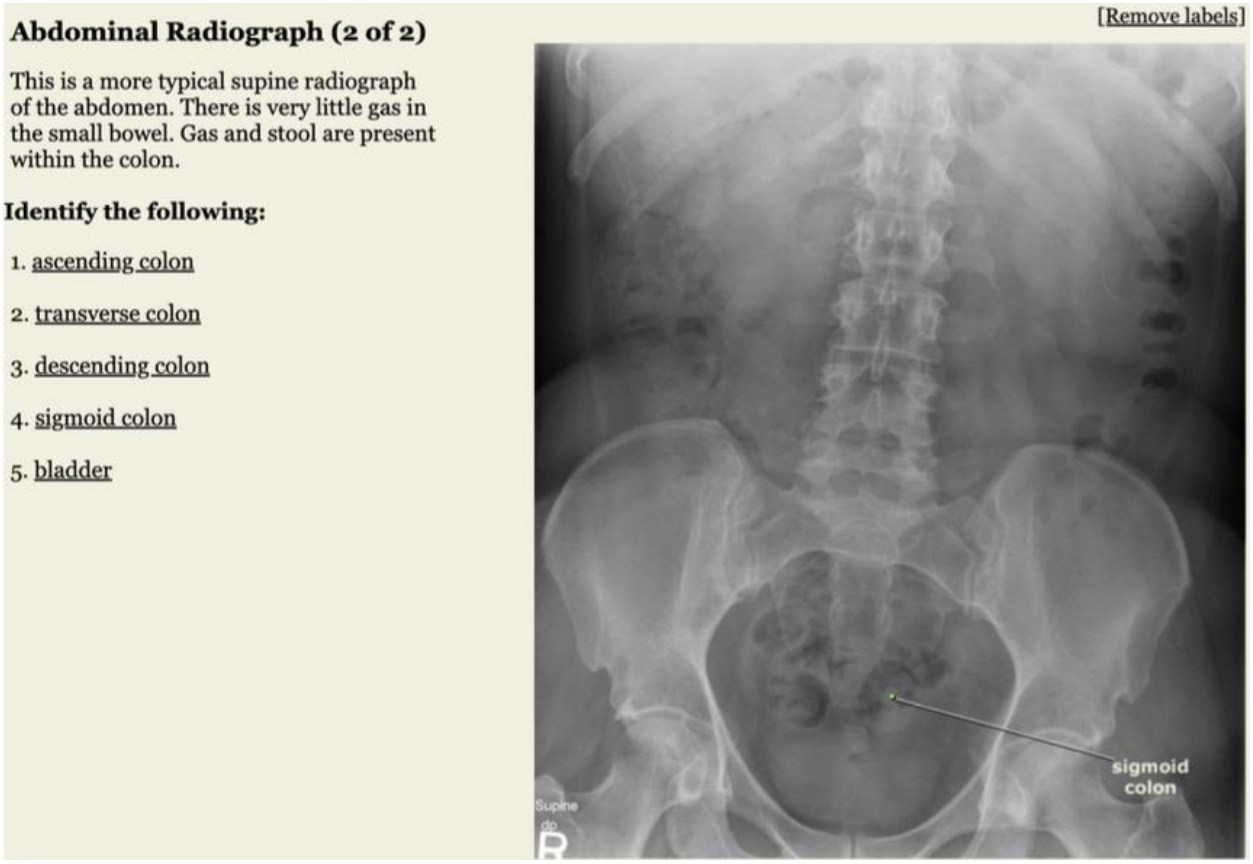

Figure 3.

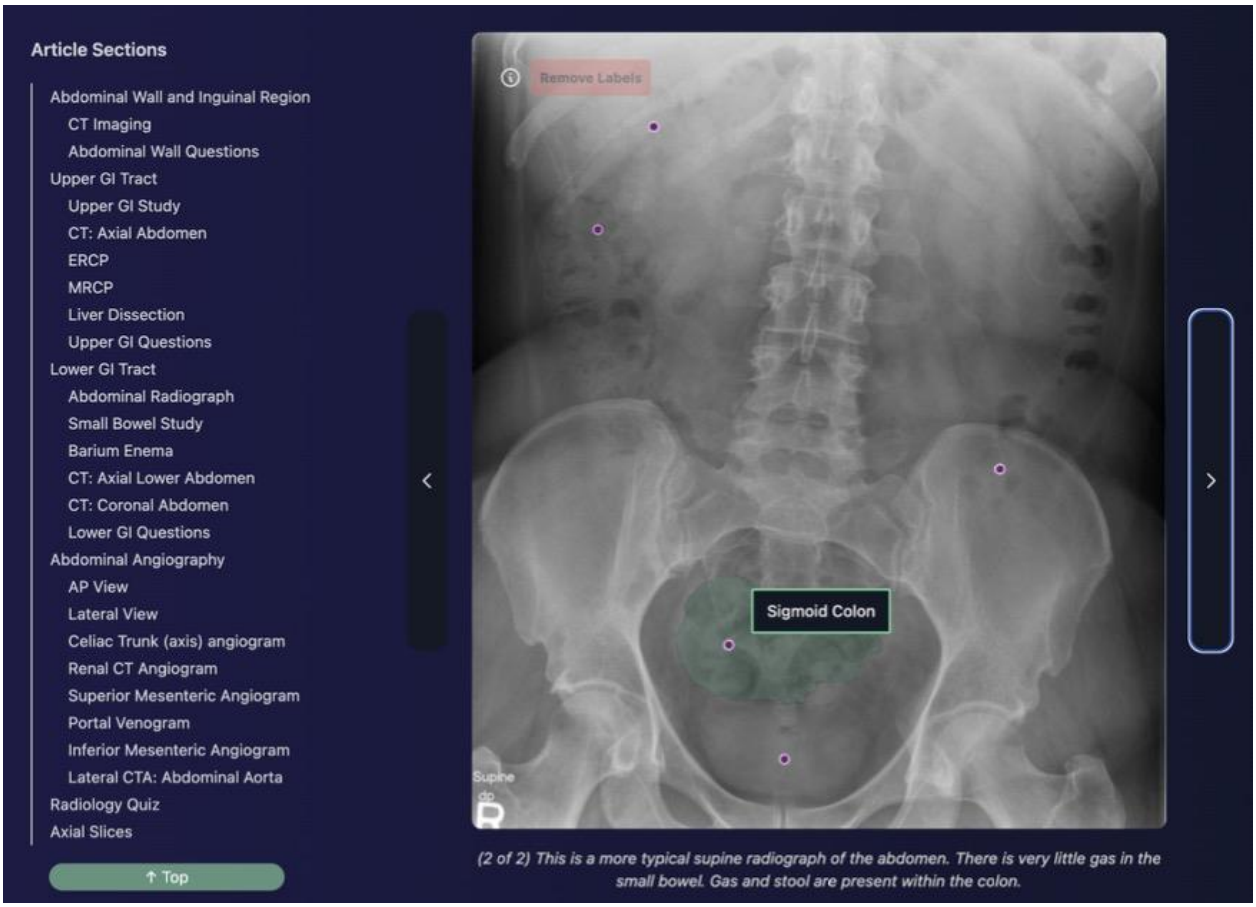
Article Sections
Abdominal Wall and Inguinal Region
CT Imaging
Abdominal Wall Questions
Upper GI Tract
Upper GI Study
CT: Axial Abdomen
ERCP
MRCP
Liver Dissection
Upper GI Questions
Lower GI Tract
Abdominal Radiograph
Small Bowel Study
Barium Enema
CT: Axial Lower Abdomen
CT: Coronal Abdomen
Lower GI Questions
Abdominal Angiography
AP View
Lateral View
Celiac Trunk (axis) angiogram
Renal CT Angiogram
Superior Mesenteric Angiogram
Portal Venogram
Inferior Mesenteric Angiogram
Lateral CTA: Abdominal Aorta
Radiology Quiz
Axial Slices
↑ Top
Remove Labels
Sigmoid Colon
Supine
(2 of 2) This is a more typical supine radiograph of the abdomen. There is very little gas in the small bowel. Gas and stool are present within the colon.

Figure 4.

Optimizing Cadaver-Based Anatomy Lab Learning for Medical Students by Providing Advanced Notice of Donor Pathology Using Post-Mortem CT Scans

Parveer Kaur, BA, BE[1], Eli Engledow, ENS, MC, USNR[1], Zach Gallaher, PhD[1], Julie Kaczmark, MD[1]
[1]University of Washington School of Medicine

Purpose:

Medical schools have begun to incorporate full-body computed tomography (CT) scans of cadavers into their curriculum. Prior to student dissection, these institutions perform CT scans of all donors used in the anatomy lab. Currently, students review imaging findings from their donor with a radiologist after completing a full-body dissection; however, there are limited studies evaluating the best method for the incorporation of clinical imaging in the gross anatomy lab. This study compares the learning outcomes of the current approach of dissection followed by CT review to an approach in which students had advanced notice of pathologic findings prior to dissections.

Methods:

31 University of Washington School of Medicine (UWSOM) first year students were surveyed: (1) after cardiovascular dissections with no additional information and (2) after abdominal dissections with advanced notice of pathology from post-mortem CT readings. Students were informed of the pathologic findings of their donor-specific CT scans via email and meetings with an expert radiologist.

The first survey examined students' understanding of gross anatomy and pathology, and if prior exposure to pathologic findings on the post-mortem CT scan would be potentially beneficial to their anatomy and pathology learning, using a 5-point Likert scale. The second survey was conducted after abdominal dissections to assess if student anatomy lab experience was impacted positively by advanced notice of CT pathology.

Results:

Without prior notification, UWSOM students identified only a fraction of the pathologies during dissections, with less than a third (29%) being recognized. After cardiovascular dissections, over 90% of students indicated they had a strong understanding of thoracic anatomy, but 37% indicated they strongly understood the pathology in their donors. Over half of these students stated that knowing the pathologies ahead of time would significantly improve their comprehension of both regional pathology and gross anatomy.

The second survey indicated over 90% of students identified a strong understanding of abdominal anatomy. 65% said they had a strong understanding of the gross pathology present in their specific donor. 23 students indicated that advanced notification of pathologies in their donor enhanced their learning of pathology, and 22 found that advanced notice of pathologies was helpful in their overall learning process.

Conclusions:

Advanced notice of pathologies identified by an radiologist on a post-mortem CT scan of anatomy donors was preferred by students. The percentage of students who had a strong understanding of anatomy post dissections remained similar, but the percentage of students who indicated a strong understanding of donor pathology increased significantly with advanced notice. Additional research is necessary considering sample size limitations, but these findings support future implementation of early post-mortem CT review into anatomy lab instruction prior to dissection.

Evaluation of Radiology Resident Proficiency in Diagnosing Vascular Conditions: A WIDI-SIM Based Study

C. David Pfaehler, BA[1], Kevin Pierre, MD[2], Cing Hoih[3], Snehith Enjem[3], Chase Labiste, MD[2], Roberta Slater, MD[2], Christopher Sistrom, MD, PhD[2], Anthony Mancuso, MD[2], Dhanashree Rajderkar, MD[2], Priya Sharma, MD[2]
[1]University of Florida College of Medicine
[2]University of Florida Department of Radiology
[3]University of Florida College of Liberal Arts and Sciences

Introduction:

Vascular emergencies present with subtle imaging findings that, when missed, may lead to devastating clinical outcomes. Diagnostic accuracy is especially important during resident-independent overnight call, where decisions often impact immediate patient management without attending oversight. Our study examines resident proficiency in detecting selected vascular conditions in a simulated on-call scenario.

Methods:

Radiology residents were evaluated using the Wisdom in Diagnostic Imaging Simulation (WIDI SIM), a computer-aided diagnostic simulation designed to replicate emergency radiology shifts. Residents interpreted 65 imaging cases, including five targeting critical vascular conditions. Each case required residents to provide a free-text diagnosis. Faculty members manually scored responses using a standardized rubric, categorizing errors as either observational or interpretive in nature. Performance was assessed based on average scores and the frequency of critical errors per case.

Results:

Across all vascular cases, the proportion of critical errors and average scores varied: Case 1 (Mycotic Aneurysm I, n=241) yielded an average score of 3.47/10, with 67% of reports containing critical errors. Case 2 (Mycotic Aneurysm II, n=194) yielded an average score of 5.68/10, with 31% containing critical errors. Case 3 (Aortic Graft Infection I, n=192) yielded an average score of 4.02/10, with 51% containing critical errors. Case 4 (Aortic Graft Infection II, n=302) yielded an average score of 8.10/10, with only 8% containing critical errors. Case 5 (Ovarian Vein Thrombosis, n=242) yielded an average score of 3.38/10, with 55% containing critical errors. Performance varied by case, with aortic graft infection in Case 4 showing the highest accuracy and the lowest critical error rate. Ovarian vein thrombosis in Case 5 demonstrated the lowest accuracy. Mycotic aneurysm in Case 1 possessed the highest critical error rate.

Discussion:

The findings of our study indicate a range of varying proficiency among residents in evaluating emergent vascular pathology on imaging. Radiographic findings of mycotic aneurysm and ovarian vein thrombosis were the most difficult for residents to identify, likely due to the subtle radiographic presentation and concurrent pathology. Missed diagnoses or misinterpretations of the

vascular pathology presented in these cases are associated with increased morbidity and mortality. These results highlight the importance of targeted educational interventions and simulation training to improve the diagnostic performance of radiology residents, especially those in preparation for independent overnight call without attending oversight.

Conclusion:

Radiology residents demonstrate variable proficiency in diagnosing vascular pathologies during simulated emergency radiology shifts, as demonstrated by WIDI SIM. The WIDI SIM is an effective tool for identifying diagnostic gaps and guiding future training. Emphasizing pattern recognition and early detection of vascular emergencies in resident education may help reduce critical diagnostic errors and ultimately improve patient outcomes.

Artificial Intelligence & Technology in Radiology

Teaching AI to Read Radiology Reports: Annotating Chest CTs for Report-Grounded Segmentation

Kent Kleinschmidt, BS[1], Mohammed Baharoon, MS[2], Michael Moritz, MD[3]
[1]Saint Louis University School of Medicine
[2]Harvard Medical School, Department of Biomedical Informatics, Rajpurkar Lab
[3]SSM-Health Saint Louis University, Department of Radiology

Introduction:

Radiology faces a convergence of increasing imaging demand, persistent workforce shortages, and a need for more efficient diagnostic communication[1]. While artificial intelligence (AI) offers the potential to improve speed and accuracy in medical imaging interpretation[2], many current systems fall short of clinical applicability because they struggle to comprehend the unstructured, nuanced, and descriptive language used in radiology reports[3–7].

This project contributes to a critical effort to develop AI systems that can "ground" these narrative descriptions in their precise anatomical locations within 3D imaging studies. By building a large, high-quality dataset that links real radiology text to volumetric chest CT segmentations, we aim to provide the necessary foundation for training and evaluating next-generation models that can function in actual clinical workflows.

Methods:

We created the ReXGrounding dataset, comprising over 1,900 chest CT scans annotated with segmentation masks representing ground truth, which refers to actual, correct segmentations by humans. We utilized RedBrick AI, a radiology annotation platform, to segment abnormal findings on chest CT scans. I annotated 259 CT scans individually, interpreting radiology reports while localizing and segmenting abnormalities within volumetric CT data (Figures 1–4). Findings ranged from discrete pulmonary nodules to complex diffuse patterns, such as ground-glass opacities. Each annotation was completed following guidelines and underwent review by an attending radiologist. These image-text pairs support the development and benchmarking of next-generation medical segmentation models, including MedSAM[2], SAT, and SegVol[3] (Figure 5). Performance was tested using DICE scores, a statistical measure of overlap between ground truth and AI model segmentation models, where higher values between 0-1 correlate with greater overlap[3].

Results:

Initial results of these efforts, as detailed in our companion study[3], demonstrate that despite fine-tuning on ReXGrounding, current models face significant challenges when attempting to localize findings described in nuanced free text, particularly for diffuse, irregular, and subtle abnormalities (Figure 6).

Discussion:

Accurately linking the complex, variable language of radiology reports to imaging features remains a major barrier to deploying AI effectively in clinical practice[3]. As imaging demand increases and radiologist shortages persist, AI systems that can assist with interpretation and communication may become essential to maintaining high-quality care[1,2]. However, as demonstrated by shortcomings of the medical segmentation models[3], these tools must be trained on clinical examples that reflect real-world diagnostic language. Clinician-guided dataset creation is therefore critical to ensure AI development aligns with practical needs and enhances clinical workflows[3,9].

Conclusion:

Our work directly contributed to the development of a robust training and evaluation resource for report-grounded medical image segmentation models. By bridging the gap between free-text radiology reporting and spatial localization in imaging, this project helps lay the groundwork for training clinically useful AI tools[3]. Such systems may become essential to manage rising imaging volumes without sacrificing diagnostic accuracy[2]. Ultimately, this work demonstrates how clinician-guided datasets can enhance the clinical relevance of radiology AI by training models on authentic language and imaging from real-world practice[3].

Figures:

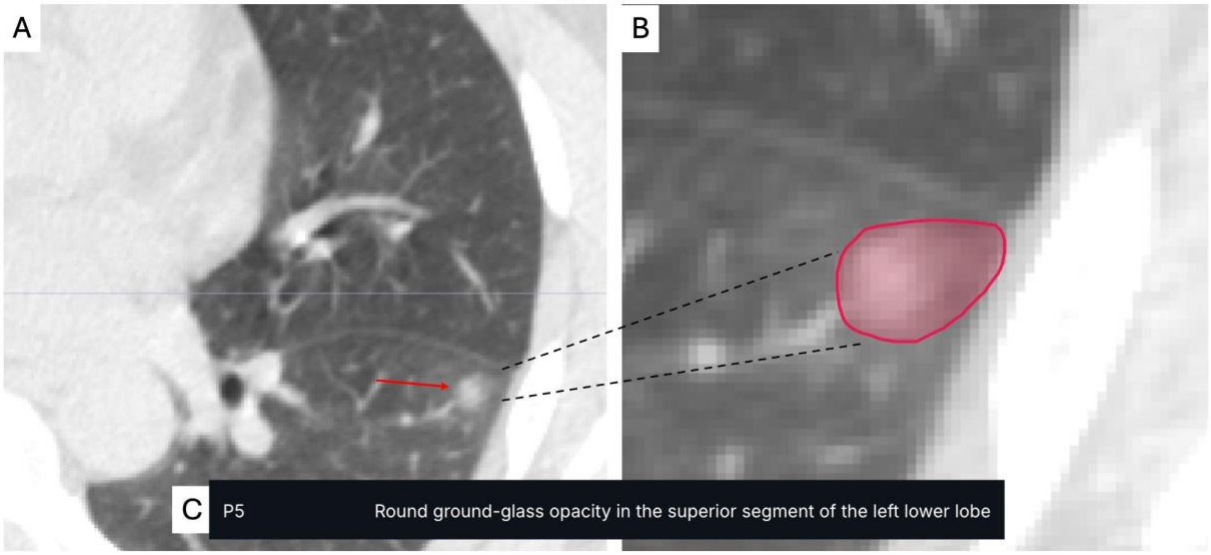

Figure 1. Axial view of CT Chest opened in the RedBrick AI annotation platform, showing a ground glass opacity in the superior segment of the left lower lobe (A), magnified and segmented in the axial view using annotation tools (B), with corresponding free-text from interpreting radiologist (C).

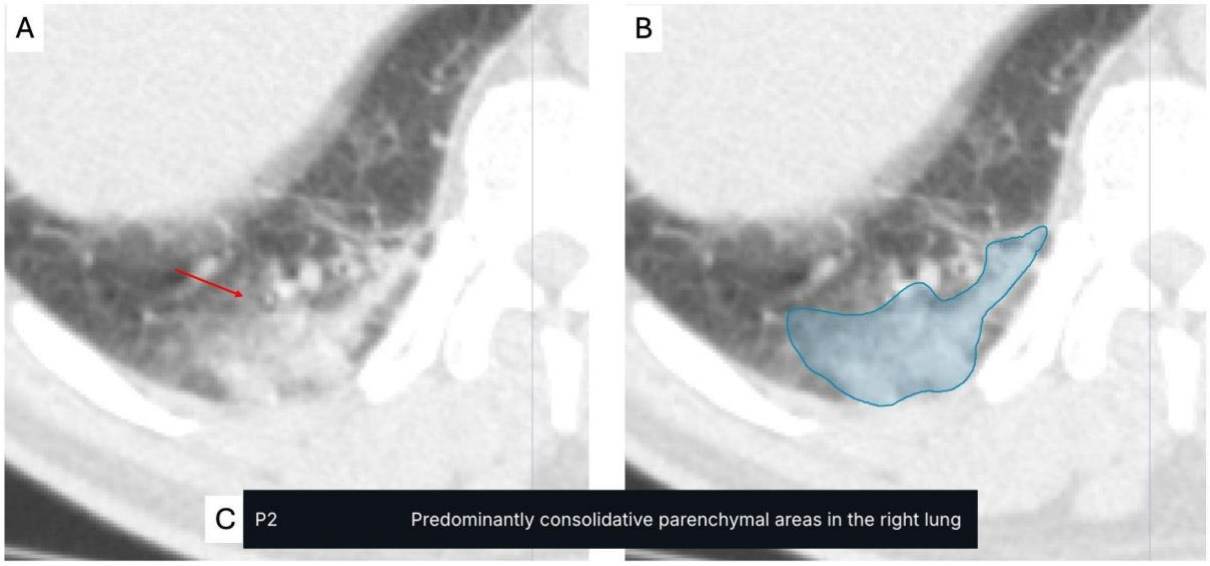

Figure 2. Axial view of CT Chest opened in the RedBrick AI annotation platform, showing areas of consolidation in the right lower lobe (A), segmented in the axial view using annotation tools (B), with corresponding free-text from interpreting radiologist (C).

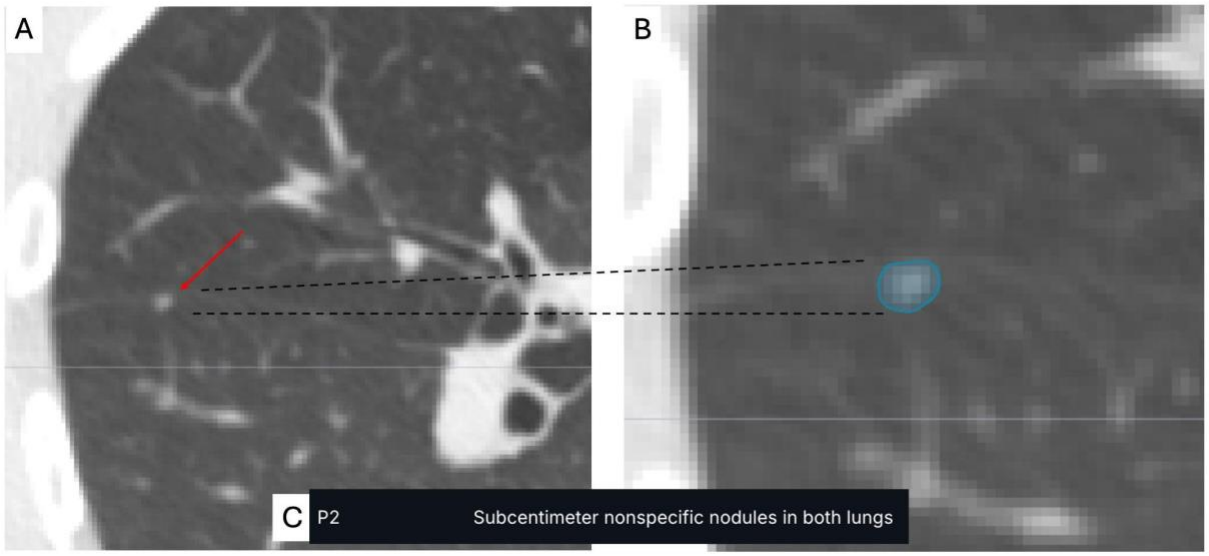

Figure 3. Axial view of CT Chest opened in the RedBrick AI annotation platform, showing a subcentimeter nodule adjacent to the oblique fissure in the right lung (A), magnified and segmented in the axial view using annotation tools (B), with corresponding free-text from interpreting radiologist (C).

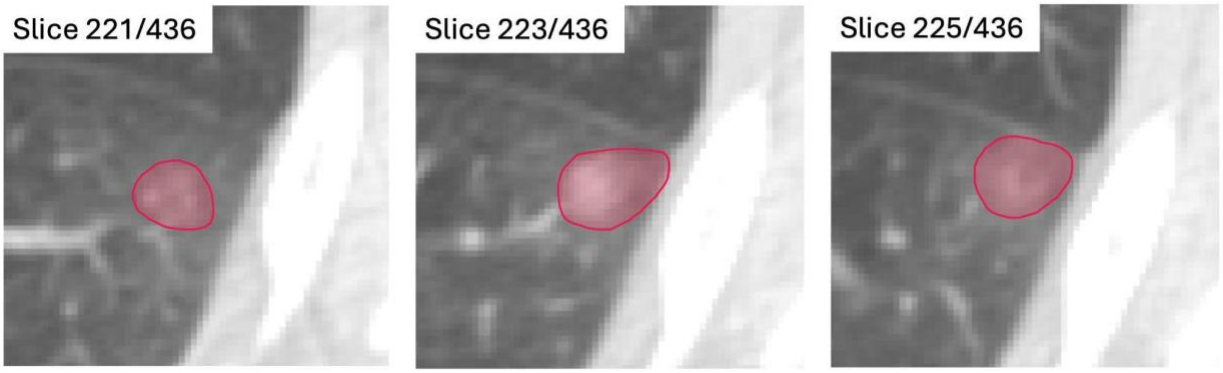

Figure 4. Consecutive slices of an axial view of a CT Chest opened in the RedBrick AI annotation platform, demonstrating 3-dimensional segmentation of a ground glass opacity in the superior segment of the left lower lobe.

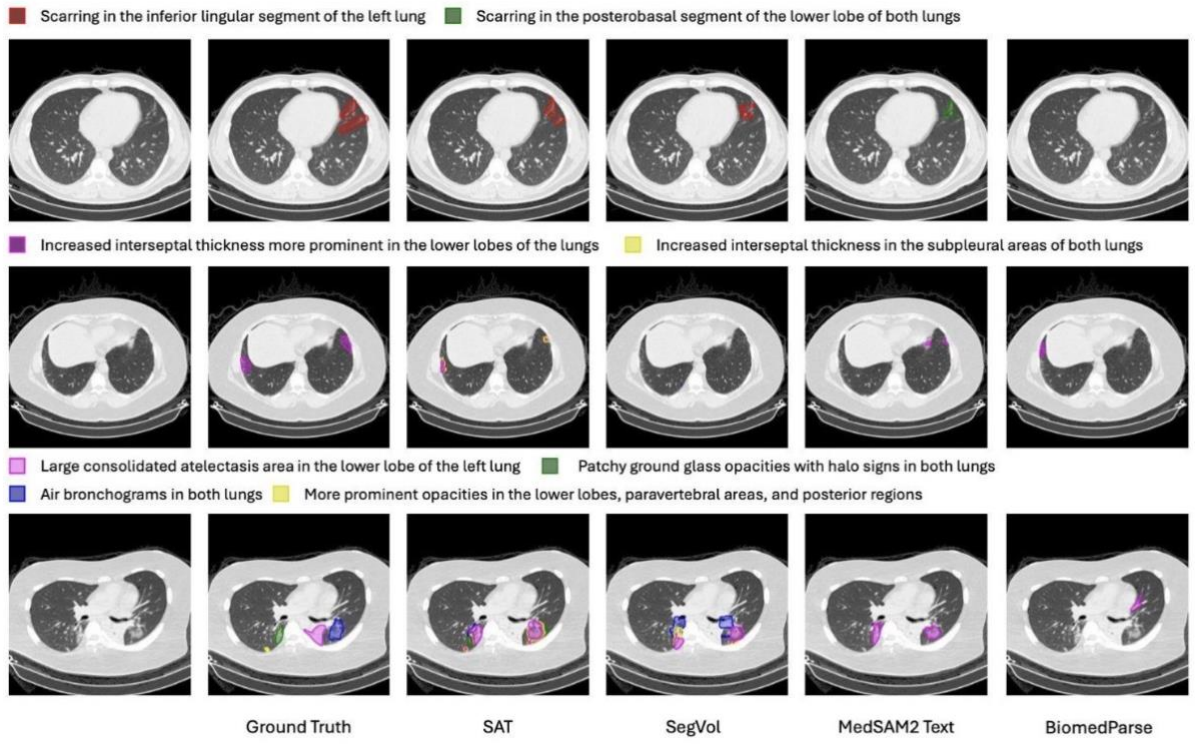

Figure 5. Visualization of segmentation examples from ReXGrounding, along with model predictions. Above each example is the text prompt given to all models, color-coded. Each row illustrates a different CT case with corresponding prompted findings and predictions from SAT, SegVol, MedSAM2, and BiomedParse.

*From MLHC companion study[3]

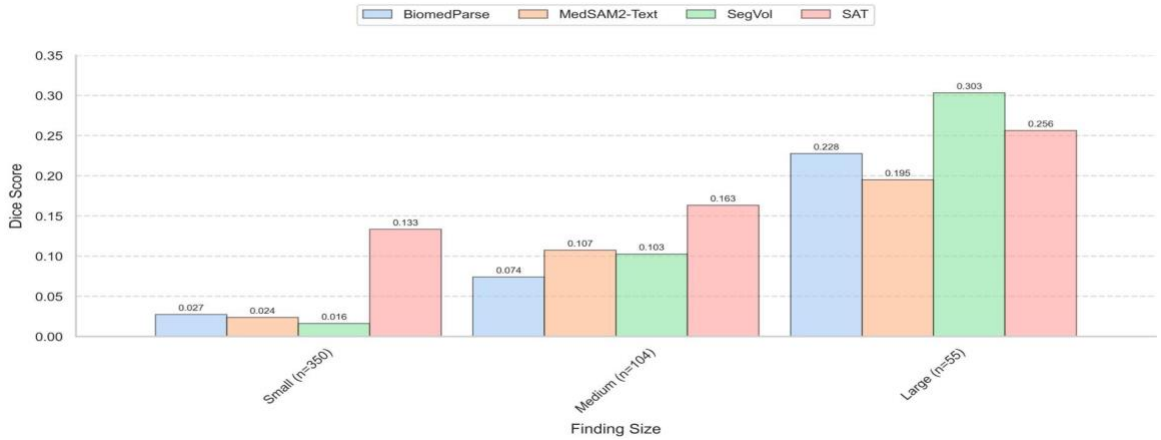

Figure 6. Segmentation performance by finding size using DICE scores. Findings were grouped into three size categories: small (bottom 50%), medium (50th to 75th percentile), and large (top 25%). All models perform better on large findings. While SegVol excels on large findings, SAT shows higher accuracy on small findings—likely due to differences in training resolution and volume downsampling strategies.

*From MLHC companion study[3]

References:

1. Rula EY. Radiology workforce shortage and growing demand: something has to give. *ACR Bulletin*. July 3, 2024. Accessed May 16, 2025. https://www.acr.org/Clinical-Resources/Publications-and-Research/ACR-Bulletin/Radiology-Workforce-Shortage-and-Growing-Demand-Something-Has-to-Give
2. Wenderott K, Krups J, Zaruchas F, et al. Effects of artificial intelligence implementation on efficiency in medical imaging—a systematic literature review and meta-analysis. *npj Digit Med*. 2024;7:265. doi:10.1038/s41746-024-01248-9
3. Bahroon M, Luo L, Moritz M et al. State-of-the-art text-prompted medical segmentation models struggle to ground chest CT findings. Preprint. Under review. *Machine Learning for Healthcare*. 2024:1–27
4. Sloan P, Clatworthy P, Simpson E, Mirmehdi M. Automated radiology report generation: a review of recent advances. *IEEE Rev Biomed Eng*. 2024. Preprint available: arXiv:2405.10842
5. Saba L, et al. Large language models for structured reporting in radiology. *Eur Radiol*. 2024;34:4212–4223
6. Müller H, et al. Automatic structuring of radiology reports with on-premise open-source large language models. *J Digit Imaging*. 2024;37(4):987–998
7. Lee J, et al. Reshaping free-text radiology notes into structured reports with natural language processing. *Radiography*. 2024;30(2):379–386
8. Reichenpfader D, Knupp J, Sander A, Denecke K. RadEx: a framework for structured information extraction from radiology reports based on large language models. arXiv:2406.15465
9. Candemir S, Nguyen XV, Folio LR, Prevedello LM. Training strategies for radiology deep learning models in data-limited scenarios. *Radiol Artif Intell*. 2021;3(6):e210014. doi:10.1148/ryai.2021210014

A Comparative Analysis between Radiologist and AI-based Volumetric Assessments of Breast Density Grading and the Potential Impact on Supplemental Screening and Costs

Jacob Devine, BS[1], Alexander Withrow, BS[1], Sabina Choudhry, MD[1]
[1]University of South Dakota Sanford School of Medicine

Introduction:

Radiologists use the Breast Imaging Reporting and Data System (BI-RADS) to categorize breast density on mammograms per 2024 Mammography Quality Standards Act (MQSA) regulations mandating breast density disclosure in every mammography report. This is crucial, as increased breast density (BI-RADS C and D) reduces cancer detection sensitivity and is an independent risk factor for breast cancer. FDA-approved AI software is now available to provide accurate, consistent breast density assessments to improve workflow and guide supplemental screening. This study examines variations between AI-based systems (Volumetric density measurement by Volpara/Lunit) and radiologist assessments, and how prospectively changing breast density classifications can impact lifetime risk estimates. Overestimation can generate increased costs and anxiety, while underestimation could delay detection of aggressive cancers in high-risk patients.

Methods:

A retrospective cohort study was conducted from March to July 2025 at Avera Health under HIPAA compliance. Radiologists assessed breast density during mammogram screenings with the ability to override the automated score. Breast density assessments were compared to prior screening mammograms or previous assessments signed in the prior 12 months. Trending was categorized as agreement or substantial change, meaning a patient had shifted to high (C or D) or low (A or B) risk. A lifetime Tyrer-Cuzick (TC) score was used to process the density measurement and guide high-risk breast clinic referrals.

Results:

Preliminary findings show that changes in breast density categories may cause confusion among providers and patients, potentially reducing compliance with screening mammograms. Miscategorized dense breasts can lead to inappropriate high-risk labeling, resulting in increased costs, radiation exposure, and false-positive biopsies. Agreement of radiologist with AI breast density grading demonstrated decreased delays in cancer detection, risk of harm from supplemental screening and treatment costs.

Discussion:

The prevalent disparities present within AI and radiologist assessments raise important clinical and economic concerns. While FDA approved AI tools offer objective and reproducible data, their utility depends upon how often the training data is refreshed and how the data can adapt across various patient populations. The inconsistency present in current AI assessments may stem from model biases, lack of generalizability, and absence of contextual clinical judgment, leading to shifts

in grading density that directly impact clinical decisions. Overestimation can result in increased psychological burden and healthcare expenditures for patients incorrectly designated as high risk. Conversely, underestimation may cause aggressive cancers to remain undetected, allowing them to progress to later stages. These findings emphasize the need for standardized protocols to mediate discrepancies between radiologists and AI assessments. Ultimately, integrating AI tools with the supervision of a radiologist could enhance diagnostic precision while preserving clinical oversight.

Conclusion:

The study comparatively analyzed the concordance between AI algorithms and radiologist assessments for breast density grading. Since machine learning tools are less effective and inconsistent without refreshed training data, lack of generalization, and training model biases, interpretations between ML and radiologist remain variable. Better agreements between assessments can promote acceptance in the breast imaging community, build patient trust, and improve workflow.

3D T2 Mapping of Medial Meniscus Extrusion at 7T Before and After Posterior Root Tear Repair

Hassan Ahad[1], Karsten Knutsen[1], Asif Hassan[1], Abdul Wahed Kajabi[1,2], Eisa Hedayati[1,2], Jutta Ellermann[1,2]
[1]Center for Magnetic Resonance Research, University of Minnesota, Minneapolis, MN
[2]Department of Radiology, University of Minnesota, Minneapolis, MN

Introduction:

Medial meniscus posterior horn root tears (MMPRTs) are significant injuries of the knee causing displacement of cartilage, leading to accelerated osteoarthritis[1]. MMPRTs are associated with meniscal extrusion, defined as radial displacement >=3 mm of the meniscus[2]. MMPRTs not treated with surgical intervention are associated with worsening arthritis and poor clinical outcomes[3]. Quantitative MRI, particularly T2 and T2* relaxation time mapping, can distinguish between normal menisci vs. torn or degenerative menisci[4]. This study focuses on 3D T2* mapping in evaluating medial meniscal extrusion between patients before and six months after surgical repair of MMPRTs, compared to healthy controls. We hypothesize that MMPRTs will increase T2* values, and that relaxation times will correlate with medial meniscus extrusion measurements taken before and after root repair.

Methods:

This study involved fifteen patients with a unilateral posterior root tear of the medial meniscus (mean age: 52 years; range: 34-62 years) and nine healthy controls (mean age: 51 years; range: 34-67 years). Each patient underwent the same MRI protocol twice using a 7T MRI system—once before repair and again six months after repair—while the control group had one scan.

The MRI protocol included T2-weighted turbo-spin echo and 3D SPACE sequences with fat suppression (Table. 1). Multi-echo T2* data were used to fit a mono-exponential signal decay through a two-parametric least-squares fitting routine in Matlab, with fitting accuracy assessed by normalizing the root mean square error (RMSE) to estimated signal intensity at an echo time of 0 ms.

Acquisition Parameter	Coronal T2 TSE FS	Axial T2 TSE FS	Sagittal T2 SPACE FS	Sagittal 3D T2* mapping
Repetition time (ms)	5750	6000	1500	26
Echo time (ms)	42	63	58	3.1, 6.1, 9.2, 12.2, 15.3, 18.4, 21.4
Flip angle (degrees)	140	140	110	15
Pixel BW (Hz/pix)	265	420	766	360
Field of view (mm^2)	129×129	140×140	150×150	130×130
Matrix size	384×307	496×347	272×272	300×300
Resolution (mm^2)	0.17×0.17	0.28×0.40	0.55×0.55	0.43×0.43
Slice thickness (mm)	2.5	2.5	0.46	1.0
Number of slices	32	41	240	120
Echo train length	8	8	47	7
Number of averages	1	1	1	1
Imaging time (min)	2:36	3:38	9:20	5:20

Table 1. MRI Parameters.

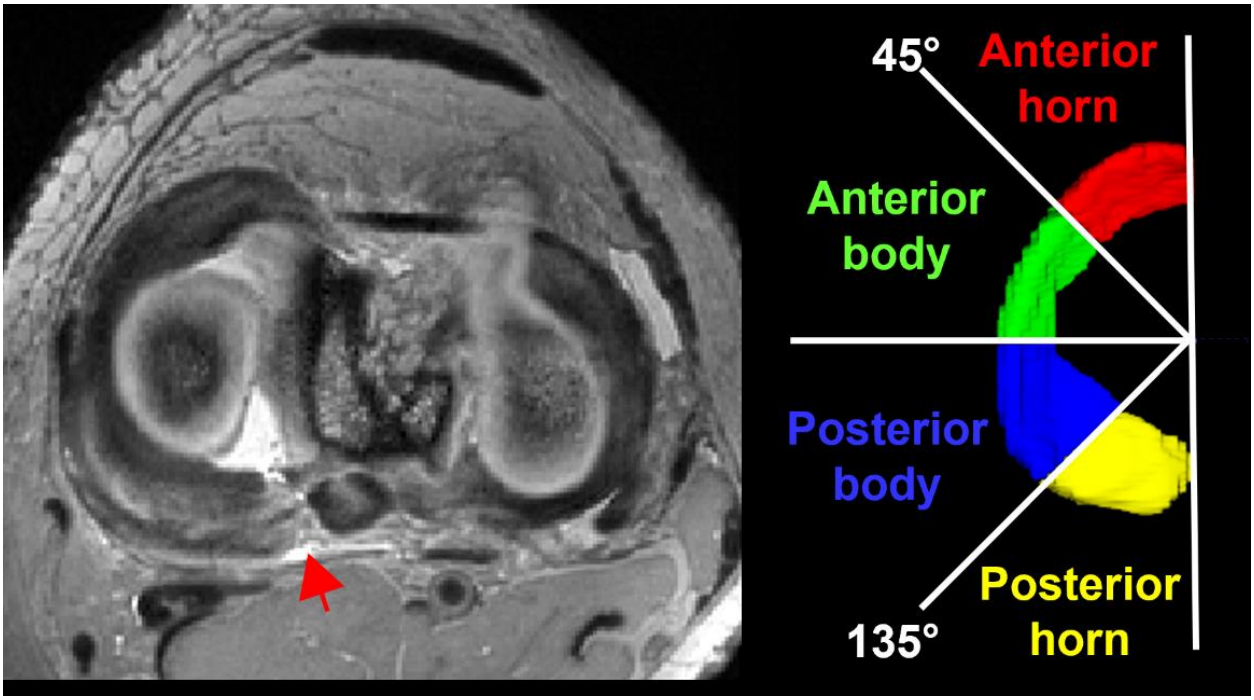

Figure 2. Left: Axial T2-weighted image showing medial meniscus posterior horn root tear (MMPRT) (arrow). Right: Regiondefinition.

Results:

Significantly longer T2* values ($p<0.05$) were observed in the medial meniscus of patients before and six months after repair of the root tear, compared to controls (Fig. 3). Post-repair patients showed significantly higher T2* values in the posterior horn of the medial meniscus compared to pre-repair patients (Fig. 4). RMSE was below 4.3% for all regions, indicating good reliability in results. Correlation analysis revealed that extrusion measurements in post-repair patients were significantly correlated with T2* values in both pre-repair ($r=0.826$; $p<0.001$) and post-repair ($r=0.732$; $p=0.002$) patients.

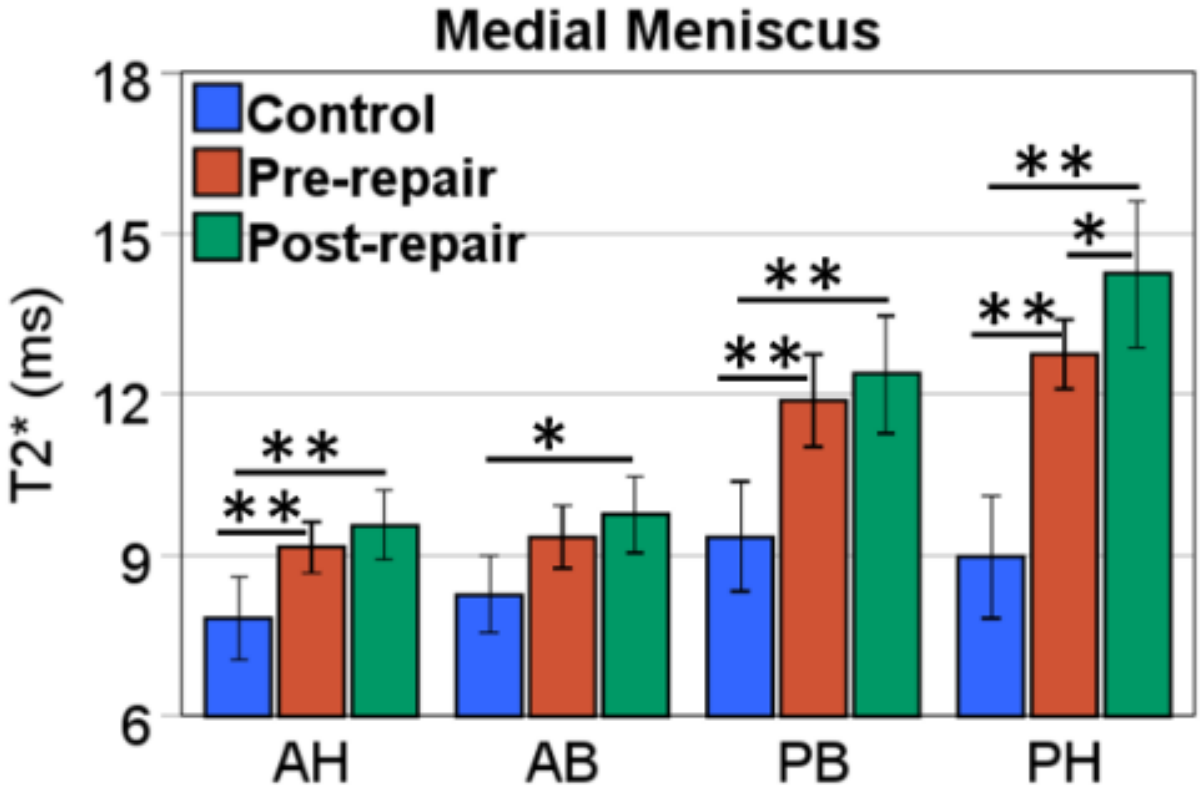

Figure 3. Bar plots comparing the T2* values of the medial meniscus in pre- and post-repair patients with MMPRTs, and healthy controls. AH=anterior horn, AB=anterior body, PB=posterior body, PH=posterior horn (PH); *$p<0.05$, **$p<0.01$.

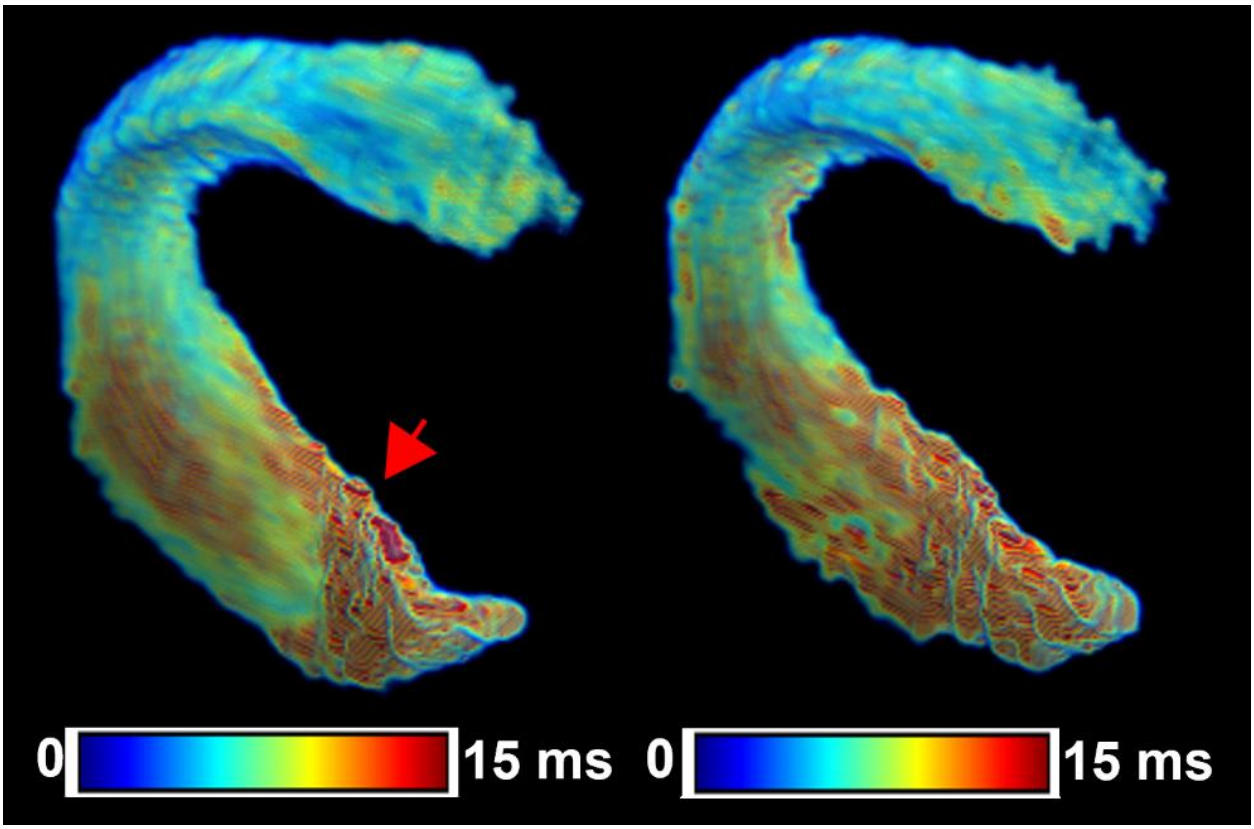

Figure 4. T2* maps before (left) and after MMPRT repair (right) show increased T2* values in areas near the tear (indicated by the arrow).

Discussion:

Elevated T2* values observed in analyzed regions of the medial meniscus in patients are suggestive of degenerative processes[5], contributing to loss of collagen organization. The findings show strong correlation between T2* mapping and meniscal extrusion, emphasizing the connection between altered structural integrity and tissue laxity.

Conclusion:

3D quantitative T2* mapping is a potent tool in evaluating meniscal extrusion in patients with MMPRTs, which can ultimately improve surgical outcomes and patient quality of life.

References:

1. Kahat DH, Nourae CM, Smith JS, Santiago CC, Floyd ER, Zbyn S, Abbasguliyev H, Kajabi AW, Ellermann JM. The Relationship Between Medial Meniscal Extrusion and Outcome Measures for Knee Osteoarthritis: A Systematic Review. Orthop J Sports Med. 2024;12(8):23259671241248457. Epub 20240809. doi: 10.1177/23259671241248457. PubMed: 39135861; PMCID: PMC11318053.
2. Langhans MT, Lamba A, Saris DBF, Smith P, Krych AJ. Meniscal Extrusion: Diagnosis, Etiology, and Treatment Options. Curr Rev Musculoskelet Med. 2023 Jul;16(7):316-327. doi: 10.1007/s12178-023-09840-4. Epub 2023 May 16. PMID: 37191818; PMCID: PMC10536705.
3. Krych AJ, Reardon PJ, Johnson NR, Mohan R, Peter L, Levy BA, Stuart MJ. Non-operative management of medial meniscus posterior horn root tears is associated with worsening arthritis and poor clinical outcome at 5-year follow-up. Knee Surg Sports Traumatol Arthrosc. 2017;25(2):383-9. Epub 20161109. doi: 10.1007/s00167-016-4359-8. PubMed PMID: 27761625.
4. Bae WC, Tadros AS, Finkenstaedt T, Du J, Statum S, Chung CB. Quantitative magnetic resonance imaging of meniscal pathology ex vivo. Skeletal Radiol. 2021 Dec;50(12):2405-2414. doi: 10.1007/s00256-021-03808-6. Epub 2021 May 13. PMID: 33938499; PMCID: PMC8536602.
5. Einarsson E, Svensson J, Folkesson E, Kestilä I, Tjörnstrand J, Peterson P, Finnilä MAJ, Hughes HV, Turkiewicz A, Saarakkala S, Englund M. Relating MR relaxation times of ex vivo meniscus to tissue degeneration through comparison with histopathology. Osteoarthr Cartil Open. 2020 Apr 3;2(2):100061. doi: 10.1016/j.ocarto.2020.100061. PMID: 33972933; PMCID: PMC7610736.

Analysis of JOCD Lesions Using 7T MRI T2* Mapping

Saumith Bachigari, BS[1], Rohan Raikar, BS[1], Abdul Wahed Kajabi, PhD[1], Brent Burg, MD[1], Marc Tompkins, MD[2], Jutta Ellermann, MD[2], Eisa Hedayati, PhD[1]
[1]Department of Radiology (CMRR), University of Minnesota, Minneapolis, MN
[2]Department of Orthopedic Surgery, University of Minnesota, Minneapolis, MN

Introduction:

Juvenile osteochondritis dissecans (JOCD) is a condition affecting children's joints, primarily the knee, caused by the failure of normal endochondral ossification[1]. This leads to localized cartilage death and potential formation of loose bone fragments within the joint[1]. JOCD is painful and, if left untreated, can result in early-onset osteoarthritis and reduced quality of life[1]. Clinical management is challenging due to the absence of standardized treatment guidelines. Physicians typically wait 3 to 18 months to observe natural healing before considering surgical intervention, such as transarticular drilling[2].

Magnetic Resonance Imaging (MRI) at 1.5T or 3T is currently used to monitor JOCD, but these conventional TSE (turbo spin echo) sequences do not effectively track lesion ossification or healing progression[2-3]. This limitation means clinical decisions are based more on symptom progression than imaging delaying necessary interventions.

Methods:

To address this, we applied a high-resolution imaging method: 3D multi-echo T2*-weighted Gradient-Recalled Echo (GRE) imaging on a 7T MRI scanner. This approach enables imaging at very short echo times (as low as 1.41 ms), allowing clearer visualization of the ossification front and differentiation between bone, lesion, interface, and cartilage. We hypothesized that changes in T2* relaxation times could serve as biomarkers for predicting whether a lesion is healing or not.

Our retrospective study included 10 femoral condyle lesions from 9 skeletally immature patients, divided into healer (5) and non-healer (4) groups. MRI data were processed to generate T2* maps using a mono-exponential decay model in Python. Lesions were segmented into four regions of interest (ROIs): parent bone, lesion, interface, and articular cartilage, using ITK-SNAP. ROIs were carefully matched across initial and follow-up scans for consistency. A control ROI set was drawn from the unaffected condyle. Median T2* values were calculated and statistically compared over time.

Results:

Results showed a statistically significant decrease in T2* values in the lesion and interface ROIs in the healer group, consistent with the conversion of soft tissues (with higher T2* values) into bone (with lower T2* values). In contrast, the non-healer group showed no significant change or even an increase in T2* values over time, suggesting a lack of ossification. The percent change in T2* values between baseline and follow-up scans were significantly different between healer and non-healer groups. Moreover, follow-up T2* values in healers approached those of control bone. We saw these changes in T2 in as little as 3 months*.

Discussion/Conclusion:

These findings suggest that T2* mapping using high-field 7T MRI can quantitatively monitor the healing trajectory of JOCD lesions. It provides a non-invasive, imaging-based biomarker to distinguish between healing and non-healing lesions months before clinical symptoms alone would suggest a course of action. This could significantly reduce the wait time for diagnosis and allow for earlier and more accurate intervention, potentially improving outcomes and quality of life for pediatric patients.

References:

1. Masquijo J, Kothari A. Juvenile osteochondritis dissecans of the knee: review. EFORT Open Rev. 2019;4(5):201–212. doi: 10.1302/2058-5241.4.180079. PMID: 31191988.
2. Kajabi AW, et al. Longitudinal 3T MRI T2* mapping of juvenile osteochondritis dissecans lesions: Pilot study. J Orthop Res. 2023;41(1):150–160.
3. Chau MM, et al. Osteochondritis dissecans: epidemiology, etiology, management, and outcomes. JBJS. 2021;103(12):1132–1151.

Acknowledgements:

National Institute of Biomedical Imaging and Bioengineering (P41 EB027061) and R01EB034575.

Dual Transfer Machine Learning (AI/ML): AI Can Detect Central Canal Stenosis Across Regions and Modalities

Zoe Rudloff[1], MS3, Bryson Hewins, MD[2], Michael Porambo, MD[3]
[1]Uniformed Services University of the Health Sciences
[2]Naval Medical Center, San Diego
[3]Walter Reed National Military Medical Center

Central cervical canal stenosis, characterized by pathological narrowing of the spinal canal leading to cord compression, affects approximately 8-11% of the U.S. adult population annually, leading to chronic pain and substantial healthcare costs exceeding $20 billion annually. Magnetic Resonance Imaging (MRI) is the current diagnostic gold standard but is expensive and less accessible than Computed Tomography (CT). Increasing CT's diagnostic capability for this condition could improve access to care, particularly in resource-limited settings.

This study explored the potential of transfer machine learning across modalities and regions of anatomic similarity. This was achieved through repurposing an existing, validated AI model from the Radiologic Society of North America (RSNA) lumbar spine degeneration challenge (2024) for fine-tuning and evaluation of a novel dataset generated from the RSNA cervical spine fracture detection dataset (2022) challenge.

The model successfully predicted SCS severity with a validation score of 0.89. The overall diagnostic accuracy, as represented by the Macro- and Micro- average Area Under the Curve (AUC), were 0.77 and 0.93 respectively. This suggests strong performance for the well-represented "normal/mild" class, which comprised 79.3% of the dataset. The higher AUC for well represented data suggests that improvement of the model relies upon increasing the representation of the moderate and severe data classes.

This research demonstrates that AI models trained on MRI images of one spinal region can effectively be repurposed to analyze CT images of a different, but anatomically similar, region. This transfer learning approach has significant implications for maximizing the utility of existing validated AI models and large open-source datasets, potentially expanding diagnostic capabilities in various healthcare settings without developing new models from scratch.